The Science of Nature (2022) 109:40
https://doi.org/10.1007/s00114-022-01810-z

ORIGINAL ARTICLE

New data on *Propyrotherium* (Mammalia, Pyrotheria) from the middle Eocene age (Chubut, Argentina): anatomy, age constraints, and phylogeny

Bárbara Vera[1] · Micaela Folino[1] · Walter Soechting[2] · Nicole Böttcher[2]

Received: 21 December 2021 / Revised: 20 July 2022 / Accepted: 27 July 2022 / Published online: 8 August 2022

Abstract

Pyrotheria is one of the most peculiar orders of South American native ungulates, whose members evolved from the early? Eocene to the late Oligocene period when they became extinct. Here, we described the most complete specimen of *Propyrotherium saxeum* ever found, one of the lesser-known representatives of pyrotheres that characterized the middle-late Eocene period of Patagonia (Argentina). It includes a nearly complete mandible and a tusk-like tooth of the same individual, as well as other isolated upper and lower teeth. *Propyrotherium saxeum* has a dental formula that includes at least P2–M3 and i2?–p3–m3 (lack of p2). It is characterized by some peculiar features of the mandible (e.g., ascending ramus longer than high, hiding the m3 and straight incisura mandibular) and dentition (e.g., cristid obliqua in p3–m3, cristid between posterior lophid and distal cingulid in m1–m3, P3–M3 and p3–m3 bilophodont, P2 and p3–m3 bi-rooted, P3–M3 three-rooted, paraconid in p3). The phylogenetic analysis reveals that *Propyrotherium* is more closely related to *Pyrotherium* and *Baguatherium*, differing from the previous hypothesis, and supports the monophyly of Pyrotheriidae including *Carolozittelia*, *Griphodon*, *Pyrotherium*, *Baguatherium*, and *Propyrotherium*. The absolute age obtained through U–Pb zircon dating of the Sarmiento Formation at Cañadón Pelado, the fossil's original locality, indicates that the fossil-bearing tuff would have been deposited between 39.65 and 40.41 Ma, with a weighted mean age of 40.03 ± 0.38 Ma (Bartonian). This implies a biochron much longer than previously thought for *Propyrotherium* and provides a chronological framework for the fauna of Cañadón Pelado.

Keywords SANU · Pyrotheriidae · *Propyrotherium* · Patagonia · Early Paleogene · U–Pb tuff age

The fauna of South American native ungulates (SANUs) includes extinct mammals that evolved within the context of South American geographic isolation during most of the Cenozoic period (Simpson 1980; Cifelli 1993). They were highly diversified, and their unique characteristics allowed them to conquer a variety of ecological niches (Croft et al. 2020). Among SANUs, the order Pyrotheria is one of the most peculiar and enigmatic groups of large-sized herbivorous mammals, although scarcely known with respect to other SANUs. Its few representatives have been recorded in the Paleogene deposits (early? Eocene–late Oligocene) of Argentina, Bolivia, Peru, Brazil, Colombia, and Venezuela. Pyrotheres include *Carolozittelia* Ameghino, 1901 (middle Eocene) and *Propyrotherium* Ameghino, 1901 (late Eocene) from Patagonia (Argentina); *Griphodon* Anthony, 1924 (?Eocene) and *Baguatherium* Salas et al., 2006 (early Oligocene) from Peru; *Colombitherium* Hoffstetter, 1970 (Gualanday Formation, Eocene) from Colombia; *Proticia* Patterson, 1977 (Trujillo Formation, Paleocene– Eocene) from Venezuela; and *Pyrotherium* Ameghino, 1888 (late Oligocene) from Argentina, Bolivia, and Brazil (Ameghino 1888, 1901; Shockey and Anaya 2004; Couto-Ribeiro and Alvarenga 2009; Couto-Ribeiro 2010; Cerdeño and Vera 2017). Two groups are commonly accepted under Pyrotheria: the Pyrotheriidae, including *Pyrotherium*, *Propyrotherium*, *Baguatherium*, *Carolozittelia*, and *Griphodon*, and the Colombitheriidae, including *Colombitherium* and *Proticia* (Kramarz and Bond 2014; Cerdeño and Vera 2017).

Communicated by: Aurora Grandal-d'Anglade

✉ Bárbara Vera
barbara.vera@comahue-conicet.gob.ar

[1] Centro de Investigación Esquel de Montaña y Estepa Patagónica (CIEMEP), CCT-Patagonia Norte, CONICET-UNPSJB, Roca 780, Esquel, Chubut 9200, Argentina

[2] SÖBÖ Geosciences, Ruta 259 km 25, Trevelin, Chubut 9203, Argentina

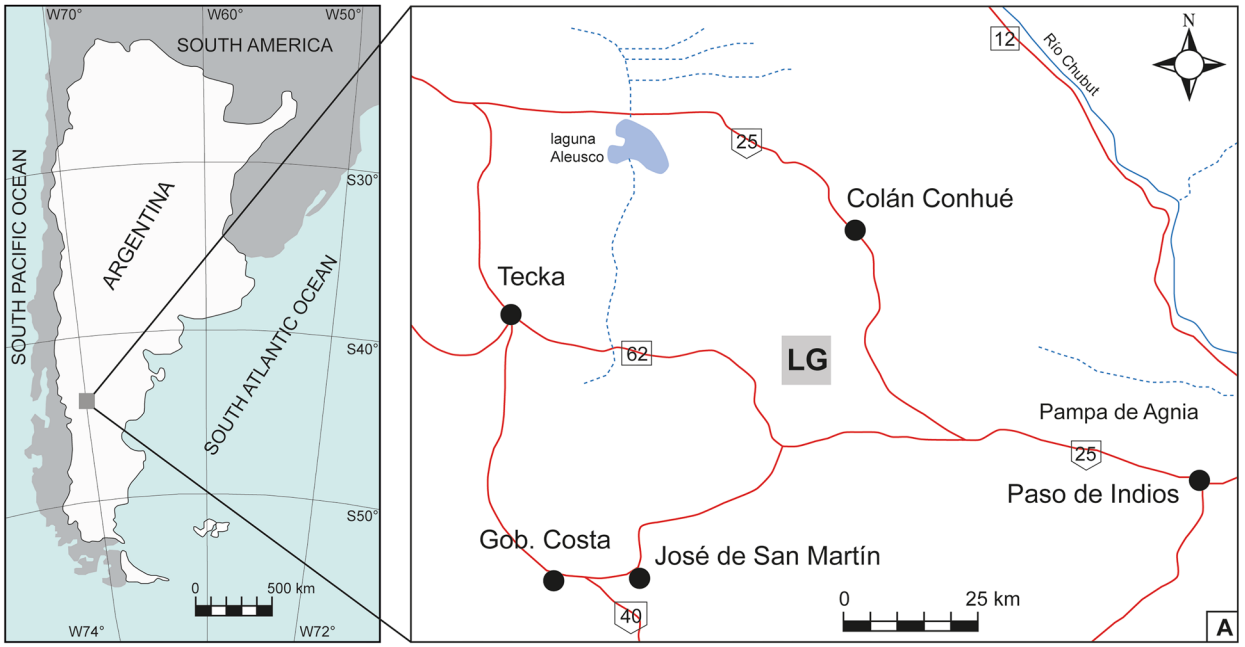
W70°
W60°
W50°
SOUTH AMERICA
SOUTH PACIFIC OCEAN
ARGENTINA
SOUTH ATLANTIC OCEAN
S30°
S40°
S50°
0
500 km
W74°
W72°
laguna Aleusco
25
12
Río Chubut
N
Colán Conhué
Tecka
62
LG
Pampa de Agnia
25
Paso de Indios
Gob. Costa
José de San Martín
40
0
25 km
A

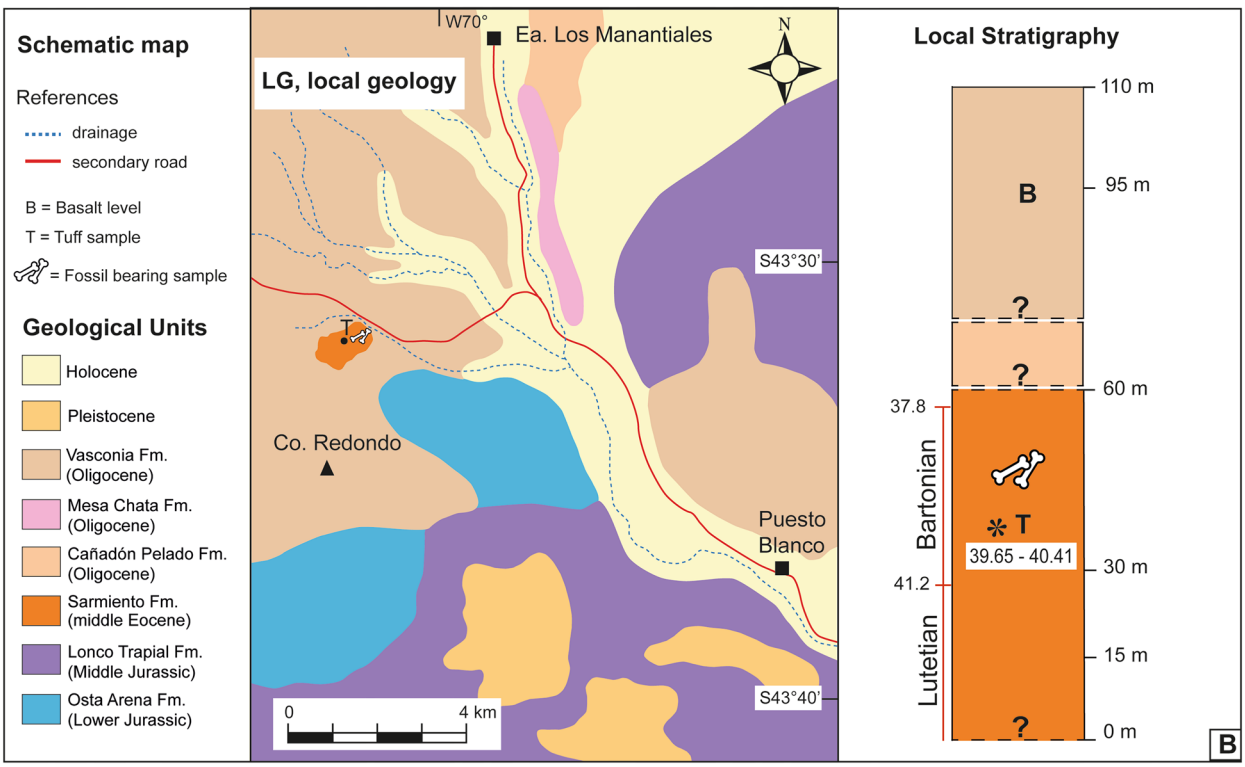
Schematic map
References
drainage
secondary road
B = Basalt level
T = Tuff sample
= Fossil bearing sample
Geological Units
Holocene
Pleistocene
Vasconia Fm. (Oligocene)
Mesa Chata Fm. (Oligocene)
Cañadón Pelado Fm. (Oligocene)
Sarmiento Fm. (middle Eocene)
Lonco Trapial Fm. (Middle Jurassic)
Osta Arena Fm. (Lower Jurassic)
LG, local geology
W70°
Ea. Los Manantiales
N
S43°30'
T
Co. Redondo
Puesto Blanco
S43°40'
0
4 km
Local Stratigraphy
110 m
B
95 m
?
?
60 m
37.8
Bartonian
T
39.65 - 40.41
41.2
30 m
Lutetian
15 m
?
0 m
B

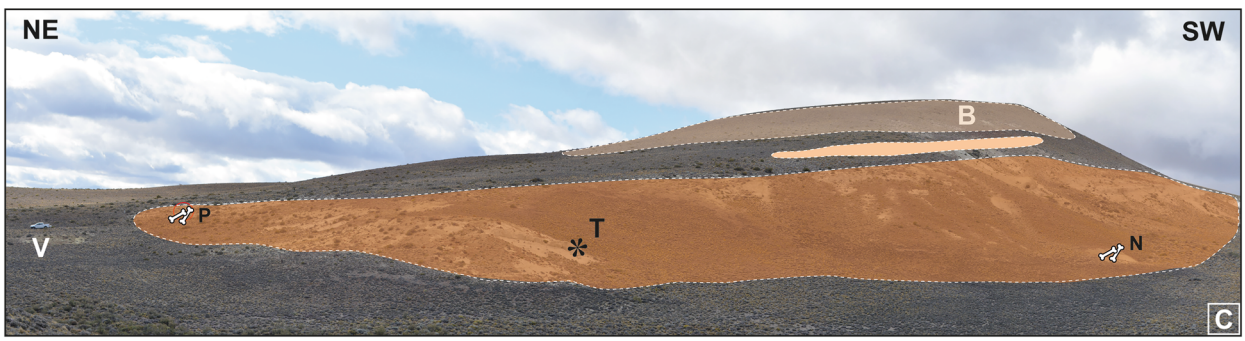
NE
SW
B
P
V
T
N
C

◂**Fig. 1** **A** Geographic location of the Cañadón Pelado area in western Chubut Province (Argentina). **B** Schematic map of the Cañadón Pelado area, showing the main geological units in the studied area, and the local stratigraphic column. **C** SE looking profile showing main units with rock and fossil samples. Abbreviations: N, *Notopithecus* level; P, *Propyrotherium* level; V, vehicle as scale

However, the hypothetical removal of *Colombitherium* and *Proticia* from Pyrotheria was proposed (see Sánchez-Villagra et al. 2000; Salas et al. 2006; Billet et al. 2010; Billet 2011; Kramarz and Bond. 2014).

One of the lesser-known representatives of pyrotheres is *Propyrotherium*. This genus, along with its only species, *P. saxeum*, was defined by Ameghino (1901) based on a few isolated teeth (a lower tusk-like tooth, a left unworn upper molar, and a lower worn molar) that C. Ameghino collected from the Mustersan fossiliferous levels of the Sarmiento Formation in Chubut Province, Argentina. However, no certain information is known about the geographic provenance of the type specimens of *P. saxeum* (Simpson, 1967; but see Kramarz and Bond, 2014). In 1904, Ameghino (1904: Fig. 198; 1906: Fig. 156) included illustrations of the cheek teeth and, after that, several authors briefly alluded to *P. saxeum*, but only minimal information was added for this species (e.g., Gaudry 1909; Scott 1913; Simpson 1945).

Many years after, Simpson (1967) identified the type material of *P. saxeum* as the lot MACN-A 10.929 composed of four likely un-associated pieces (probably a left P4; a lower cheek tooth, p4 or m1; a lower tusk; and a fragment of upper tusk) and he designed the P4 as the lectotype. In addition, Simpson attributed 30 specimens, primarily collected in Cerro Talquino (Chubut Province), to the genus *Propyrotherium* and highly likely to *P. saxeum* and provided a diagnosis for this species although describing with some uncertainties the characteristics of the P3–M3 and p2–m3 series. More recently, Kramarz and Bond (2014) reanalyzed the type material, those specimens reported by Simpson (1967), and other isolated teeth coming from several localities of the central portion of Chubut Province. Based on that, Kramarz and Bond (2014) reconstructed the cheek teeth formula of *P. saxeum* as P2–M3/p2–m3, interpreting some features and providing an emended diagnosis for this species.

Here, we describe the most complete mandible with an associated tusk-like fragment of the same individual, as well as upper and lower isolated cheek teeth attributed to *Propyrotherium saxeum*. These specimens were found in situ in a small Cenozoic outcrop at Cañadón Pelado, a new Paleogene fossil locality from the western portion of Chubut Province. These new remains and rock samples from the tuff levels at Cañadón Pelado allow us to (1) greatly improve the diagnosis of *P. saxeum*, verify its dental formula, and describe new characteristics for this taxon, (2) re-examine specimens (lower and upper isolated teeth) previously referred to *P. saxeum*, (3) perform a new phylogenetic analysis and evaluate its relationships with other pyrotheres, (4) obtain absolute ages for a tuff level at a Cañadón Pelado locality, and (5) establish correlations with other calibrated middle-late Eocene units from Patagonia and other areas of Argentina.

Geographic location and geological settings

Compared to the eastern area (i.e., San Jorge Basin), the western Chubut Province is characterized by its geological complexity and almost unexplored and little-known Cenozoic outcrops. For this region, the literature is predominantly devoted to the upper Paleozoic and Mesozoic sediments but lacks a consensus on the Cenozoic stratigraphy (e.g., Feruglio 1949; Suero 1948, 1953, 1958; Lesta and Ferello 1972; Chebli et al. 1976; Nullo 1983; Silva Nieto et al. 2005). Both the Serie Andesítica and Sarmiento Formation were mentioned as being equivalent in different parts of central-western Chubut (see Lesta and Ferello 1972), but the scarce reports of mammal fossils and dating enabled the correlation between the Serie Andesítica and the Sarmiento Formation in its type locality from the San Jorge Basin (Pascual and Odreman Rivas 1973). For example, Lesta and Ferello (1972) described three tuffaceous levels in Pampa de Agnia: a yellowish muddy lower level with nests of fossil vespids, a white-yellowish level with mammal bones, and the upper level that they identified as belonging to the Sarmiento tuffs. In the same area, Nullo (1983) identified sediments of the Sarmiento Formation and divided the formation into two subunits: the lower level being white-yellow and distinctly clastic and the upper subunit with tuffaceous characteristics, light brown-to-brown colored, but no mammal fossils were reported. Furthermore, Pascual and Odreman Rivas (1973) mentioned mammal bones in El Pajarito, 30 km east of Pampa de Agnia, but no details were reported except they were probably from the Deseadan age.

The fossiliferous site studied in this research (43° 32′ 20.50″ S, 70° 2′ 32.50 ″ W) is in the Languiñeo Department, west-center of Chubut Province (Argentina; Fig. 1A), 130 km from Esquel City via the national route No. 25 through Pocitos de Quichaura (Fig. 1B). The area is crossed by the Pelado creek (Fig. 1C), which defines the homonymous Cañadón Pelado Formation (Turner 1983). We use the Cañadón Pelado name to identify the new fossiliferous site as well. The Cañadón Pelado Formation is composed of conglomerates, sandstones, and tuff (Turner 1983), whose early Oligocene age was assigned based on field relationships with the underlying Paleocene-Eocene units (e.g., Tepuel Group and La Cautiva Formation) and the overlying Oligocene formations (e.g., Meseta Chata and La Vasconia; see Silva Nieto et al. 2005). The only fossils reported from the Cañadón Pelado Formation correspond to wood and leaf

remains, which were found in an area south of the type locality of this unit (Franchi and Page 1980).

The recent discovery of mammal bones (Taboada A personal communication) in tuffaceous sediments outcropping on a gentle slope, 10 km south-west from the type locality of the Cañadón Pelado Formation (Fig. 1B), led to further explorative work, and the results of which are the focus of this present contribution. Through the field trips carried out in the Cañadón Pelado locality during three consecutive spring seasons, from 2016 to 2019, more than two hundred vertebrate fossil remains (attributed to SANUs, xenarthrans, and marsupials) were collected from a subhorizontal layer of tuff and tuffaceous sandstones, where we recognized two fossil mammal bearing stratigraphic levels with fossils in situ (see P and N in Fig. 1C). A preliminary study of the mammal remains allowed for the identification of at least two well-distinguished mammal assemblages with affinities to the Casamayoran (Barrancan) and Mustersan South American Land Mammal ages, encompassing a middle-late Eocene age (González Ruiz and Vera 2018; Vera et al. 2020a, b).

It should be noted that these tuffaceous sediments, probably due to their scarce exposure, have not been previously recognized in the area and were mapped as the La Vasconia Formation (Silva Nieto et al. 2005). This formation is a unit of basalt flow widely distributed in the western region of the Chubut Province (Nullo 1983). Precisely, in Pampa de Agnia, located 40 km approximately southeast of the Cañadón Pelado site (Fig. 1A), Nullo (1983) attributed a late Oligocene age to the La Vasconia Formation. This author based his assumption on the fact that the basalt intercalates and covers the underlying sediments of the Sarmiento Group (sic), which bears, according to several authors, abundant mammal fossils of the Deseadan age in nearby areas (e.g., Pascual and Odreman Rivas 1973; Chebli et al. 1976).

Thus, based on the mammalian content, and also the lithological composition and the antecedents in nearby areas concerning stratigraphic relationships with the upper and lower rocks, we regard the tuffaceous sandstone at Cañadón Pelado as belonging to the western facies of the Sarmiento Formation.

Institutional abbreviations ACM, Amherst College Museum, Amherst, Massachusetts, USA; AMNH FM, American Museum of Natural History, Fossil Mammals, New York, USA; FMNH P, Field Museum of Natural History, Paleontology, Chicago, USA; LIEB-PV, Colección Paleovertebrados, Laboratorio de Investigaciones en Evolución y Biodiversidad, Esquel, Argentina; MACN-A, Museo Argentino de Ciencias Naturales "Bernardino Rivadavia," Colección Ameghino, Buenos Aires, Argentina; MPEF, Museo Paleontológico "Egidio Feruglio," Trelew, Argentina; MLP, Museo de La Plata, La Plata, Argentina.

Other abbreviations I1/i1, first upper/lower incisor; I2/i2, second upper/lower incisor; I3/i3, third upper/lower incisor; C/c, upper/lower canine; TD, transverse diameter; H, height; L, length; P1/p1, first upper/lower premolar; P2/p2, second upper/lower premolar; P3/p3, third upper/lower premolar; P4/p4, fourth upper/lower premolar; M1/m1, first upper/lower molar; M2/m2, second upper/lower molar; M3/m3, third upper/lower molar; SALMA, South American Land Mammal Age.

Materials and methods

Dating methodology Approximately 2 kg of rock sample was obtained from a tuff level 15 m below the *Propyrotherium* bearing level. The U/Pb analyses were carried out at LA.TE ANDES S.A. Laboratory (Vaqueros, Salta, Argentina). The zircon concentrates were obtained using gravimetric, magnetic, and optical techniques. The analyses were performed with an instrumental combination of LA-ICP-MS (laser ablation–inductively coupled plasma-mass spectrometry). U/Pb ages were calculated from isotopic ratios using 91,500 zircons as reference material (Wiedenbeck et al. 2004) and repeated measurements on Plešovice zircon standard (TIMS reference age 337.13 ± 0.37 Ma; Sláma et al. 2008).

The information on the analytical conditions, as well as the recommended age (Ma) based on 206Pb/238U relationships for ages less than 1.5 Ga and the 207Pb/206Pb relationships for ages greater than 1.5 Ga (Gehrels et al. 2008) are presented (SI1). The calculation of the discordance between the ages of 207Pb/235U is shown in Appendix 2. For the graphs of relative probability, calculated means, and Concordia ages, only the values with a disagreement of less than 10% were taken (SI2).

The time scale used in the text is based on the International Stratigraphic Chart (Cohen et al., 2022).

Systematic study We compare the new specimens of Cañadón Pelado to the type specimens of *Propyrotherium saxeum*, as well as other specimens attributed to the same genus and/or species and other members of Pyrotheria. *Pyrotherium romeroi* Ameghino, 1888 (ACM 3207, FMNH P 12,987, MACN-A 52–292, MACN-A 11.747; Gaudry 1909; Loomis 1914; Billet 2010); *Pyrotherium macfaddeni* Shockey and Anaya, 2004; *Carolozittelia tapiroides* Ameghino, 1901 (MACN-A 10666); *Proticia venezuelensis* Patterson, 1977; *Colombitherium tolimense* Hoffstetter, 1970 (Billet et al. 2010); *Griphodon peruvianus* Anthony, 1924 (Patterson 1942); and *Baguatherium jaureguii* Salas et al., 2006. We also compare specimens of the Xenungulata *Carodnia* (Simpson 1935; Paula Couto 1952; Gelfo

et al. 2008; Antoine et al. 2015; Vera et al., 2020a) and the Notoungulata *Notostylops* (MACN-A 10499, AMNH FM 28,634; Simpson 1948).

For lower and upper cheek teeth, we use mesial/distal and labial/lingual for differentiating the features (e.g., cingulae/cingulids, tubercles, faces) present in each loph/lophid. In the case of incisors, we use anterior/posterior and dorsal/ventral for describing the facets oriented concerning the anteroposterior axis of the skull. In upper check teeth, protoloph refers to the crista joining paracone with protocone in the anterior loph, while metaloph refers to the crista joining the metacone with hypocone in the posterior loph. In lower cheek teeth, metalophid refers to the cristid joining protoconid with metaconid in the anterior lophid, while entolophid refers to the cristid joining the hypoconid with entoconid in the posterior lophid.

We take dental measurements using a digital caliper: length (L), as the maximum value measured anteroposteriorly; and width (W), as the maximum value measured labiolingually. In the case of the width, we measure two independent values considering the anterior lophid (aW) and the posterior lophid (pW).

We perform a phylogenetic analysis coding 33 morphological characteristics (including characteristics of the mandible bone and upper/lower teeth) for nine taxa (SI3). Most of the characteristics are essentially new except for five of them that were taken from previous authors (Salas et al. 2006; Kramarz and Bond 2014; Antoine et al. 2015). We include all the pyrotheres at the generic level (seven genera) and a Xenungulata (*Carodnia*) and a Notoungulata (*Notostylops*) as the outgroup (SI4). We use TNT 1.5 (Goloboff et al. 2008) and Mesquite 3.6 (Maddison and Maddison 2018) software. All characters were treated as unordered. We assumed maximum parsimony under equal weights and conducted heuristic searches with the tree bisection reconnection swapping algorithm (TBR), using 1000 random addition sequences and saving 10 trees per round. Support values were assessed using Bremer and jack-knife indices, and nodal support was estimated using the script BREMER. RUN provided by TNT, GC frequency, and symmetric resampling (Goloboff et al. 2003).

Results

Geology and geochronology data

The sequence of the Sarmiento Formation at Cañadón Pelado, with an estimated thickness of 60 m, corresponds to a medium to coarse, monomictic dacitic tuff with partial spherulitic textures. It is a friable rock, without evidence of grain sorting (i.e., no evidence of reworking). The dated tuff sample was taken 15 m below the fossiliferous level bearing the *Propyrotherium* specimens (Fig. 1B). Above the exposed section of the Sarmiento Formation, a 10-m-thick fluvial sandstone level was identified that could correspond to the Cañadón Pelado Formation, which was mapped in the area as well (Silva Nieto et al. 2005). However, this section is barely exposed in the profile and is covered by the basalts of the La Vasconia Formation (a widely distributed lava flow); thus, an impediment identifies its contacts (Fig. 1B).

The geochronology results of the tuff sample show that 28 of 69 analyzed samples yielded 90 to 110% concordant data of ages (those with disagreement less than 10%), which encompasses from 44.1 to 37.5 Ma, with a weighted mean 206Pb/238U date of 40.03 ± 0.38 Ma and a near-optimal MSWD ($=0.035$; SI1-2). This dating is interpreted as corresponding to the sampled tuff deposition, which correlates to volcanic events that took place during mid-Lutetian and Bartonian periods (or ages) (see Silva Nieto et al. 2005 and its respective references).

Systematic palaeontology

Order PYROTHERIA Ameghino, 1894
Family PYROTHERIIDAE Ameghino, 1894
Genus *PROPYROTHERIUM* Ameghino, 1901
Propyrotherium saxeum Ameghino, 1901
Figures 2–4

Lectotype MACN-A 10.929, left P4 (Ameghino 1904: Fig. 198; Ameghino 1906: Fig. 156A; Simpson 1967: pl. 45, Fig. 2; Kramarz and Bond, 2014: Fig. 2A).

Paralectotype MACN-A 10.929, left p4 and fragments of tusks (Ameghino 1906: Fig. 156B-C; Simpson 1967: pl. 45, Fig. 6; Kramarz and Bond 2014: Fig. 3A).

Type locality Unknown (but see Kramarz and Bond 2014).

Referred specimens LIEB-PV 3200, two fragments of the right mandible, one preserving symphysis and the p3–4, and the other with m2–3; left mandible with p3–m3; root fragment of lower left tusk-like teeth (i2?), and fragment of zygomatic arch. LIEB-PV 3201, a right m1. LIEB-PV 3202, a right P3. LIEB-PV 3208, a left P2. AMNH FM 29,391, a right ?P3. AMNH FM 29,393, a right m3. MLP 55-III-10-1a, a right M1 or M2. MLP 55-IX-28-1a, a left M1 or M2. AMNH unnumbered (labeled as "O3"), a right M3.

Localities Specimens housed at LIEB come from Cañadón Pelado, western Chubut Province (Fig. 1); specimens housed at AMNH come from Cerro Talquino, central Chubut Province (see Simpson 1967); specimen housed at the MLP

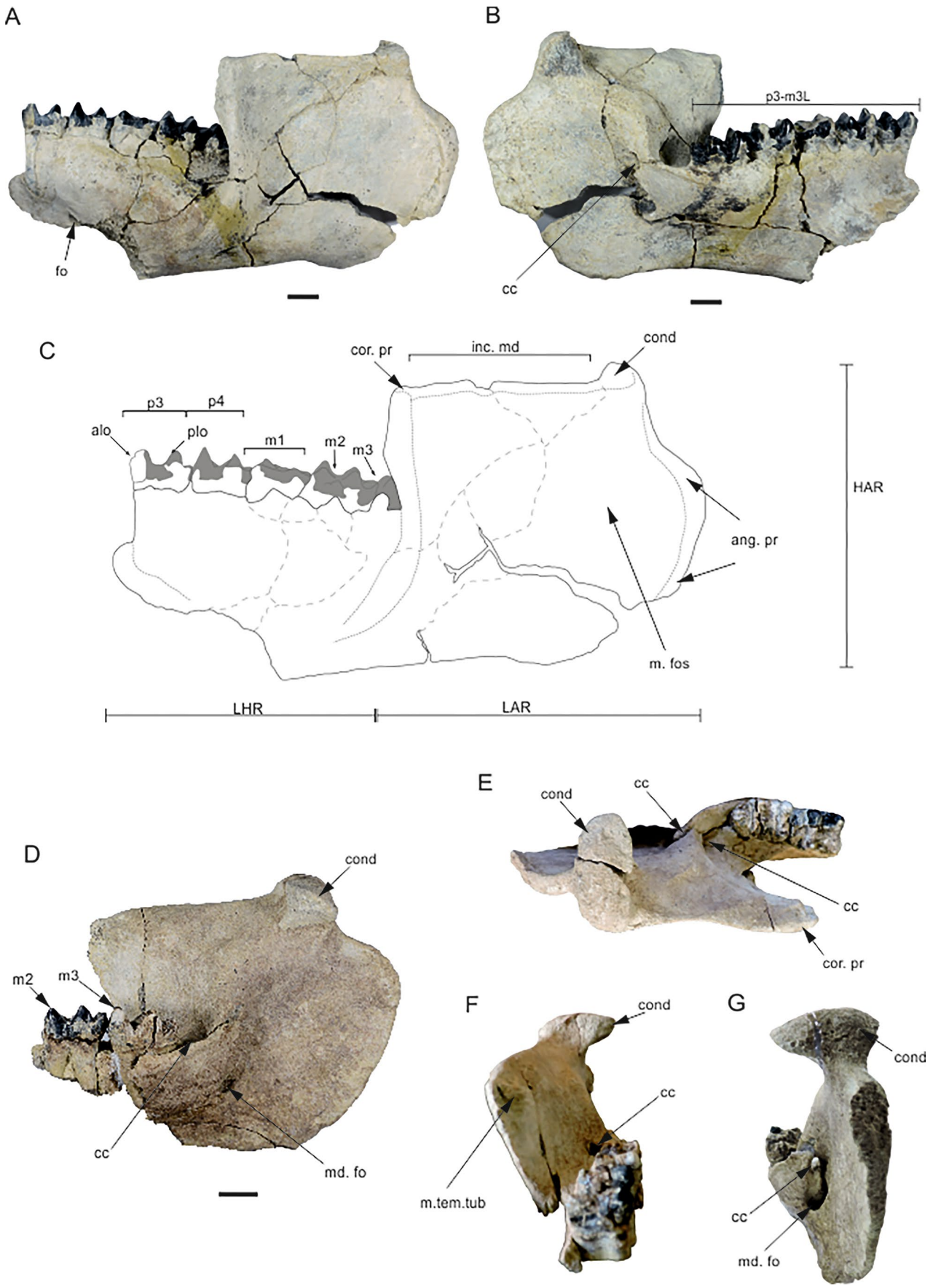
A
fo
B
p3-m3L
cc
C
cor. pr
inc. md
cond
p3
p4
alo
plo
m1
m2
m3
ang. pr
HAR
m. fos
LHR
LAR
D
cond
m2
m3
cc
md. fo
E
cond
cc
cc
cor. pr
F
cond
cc
m.tem.tub
G
cond
cc
md. fo

◂**Fig. 2** *Propyrotherium saxeum*. LIEB-PV 3200: **A**–**C** left mandible fragment with p3–m3 in lateral (**A**) and medial (**B**) views, and schematic lineal drawing (**C**); **D**–**G** right mandible fragment, preserving m2–m3 in medial (**D**), dorsal (**E**), anterior (**F**), and posterior (**G**) views. Abbreviations: alo, anterior lophid; ang. pr, angular process; cc, coronoid canal; cor. pr, coronoid process; cond, mandibular condyle; fo, foramen; HAR, height ascending ramus; inc. md, incisure mandibular; L, length; LHR, length of the preserved portion of the horizontal ramus; LAR, length of the ascending ramus; m. fos, masseteric fossa; md. fo, mandibular foramen; m. tem. tub, tuberosity for *m. temporalis*; plo, posterior lophid. All scale bars represent 20 mm (**C**, **E**–**G**, not at scale)

comes from Sierra Chaira, and the remaining localities indicated by Kramarz and Bond (2014) from central Chubut Province.

Geologic unit and age Sarmiento Formation (Chubut Province, Argentina): Bartonian, 40.03 Ma for Cañadón Pelado locality in this paper; Mustersan SALMA (late Eocene period; Ré et al. 2010) for most of the MLP and AMNH specimens; and tentatively Tinguiririan SALMA (early Oligocene; Ré et al. 2010) based on a single specimen (see Kramarz and Bond 2014); and Las Chacras Formation (Río Negro Province, Argentina): Bartonian, 39.2 ± 2 Ma (Kramarz et al. 2022).

Remarks In spite of the subtle differences, mostly given by wear, and the limited type material, we do recognize a close morphometric similitude between the new specimens LIEBPV 3200, 3201, and 3202 from Cañadón Pelado and the type specimens of *P. saxeum* (MACN-A 10.929), which allow us to attribute all of them to the same species (see below).

Emended diagnosis (modified from Kramarz and Bond 2014) Mandible with coronoid canal; longer than high ascending ramus, laterally hiding the m3, and with a straight incisura mandibular. The dental formula includes at least the P2–M3 (uncertain upper incisors, canine, and P1) and /i2?–p3–m3 series (lacking p2). i2? with circular section and laterally divergent. P2 with triangular contour and three blunt cones. P3–M3 and p3–m3 bilophodont. P2 and p3–m3 bi-rooted. P3–M3 three-rooted (one lingual and two labials). P3–M3 with mesial and lingual cingula, and M3 with distal cingulum. M1–2 with slightly to moderately curved lophs, and M3 with moderately curved anterior loph and extremely curved posterior loph. Anterior loph/id labio-lingually narrower than the posterior loph/id in P3–4/p3–4, sub-equal in M1–2/m1–2, and opposite relation in m3. Nearly parallel lophids in p3–4 and m3, and divergent in m1–2. Distinct paraconid and paralophid in p3, and p4 are similar to molars. Thin mesial cingulid in m1–2 and variably present in m3; thin labial cingulid in p3–m3; and conspicuously developed distal cingulid which increases in size from p3 to m3 where forms an expanded shelf. A cristid obliqua connecting lophids on p3–m3, and a longitudinal cristid extending from the posterior lophid to the distal cingulid in m1–m3. Labial and lingual tubercles in the central valley variable present in lower check teeth, and labial tubercle variable present in upper cheek teeth. Crenulated surfaces on lower and upper cheek teeth.

Description and comparisons

Mandible In the left hemimandible LIEB-PV 3200 (Fig. 2A, B), the horizontal ramus is shorter in comparison to the length of its ascending ramus (see below; Fig. 2C) and low relative to the m1–3 series length (L = 92.9 mm; Fig. 2B). Between the p3 and m3, the horizontal ramus height decreases from > 90 mm (at the p3 level) to 68.8 mm (at the m3 level) (Fig. 2B). The deepest point of the mandible occurs at the symphysis (Fig. 2B), a feature also described for *Proticia* (Patterson 1977). The left hemimandible, although incomplete, has a length of 297.2 mm from the most anterior border ahead of p3 to the most posterior border of the angular process (LHR + LAR; Fig. 2C). There is a rounded and large mandibular foramen below p4 (Fig. 2A). The foramen is located between p4 and m1 in *Griphodon*, while its position and presence are variable in *Pyrotherium* (Anthony 1924; Patterson 1942; Billet et al. 2010). The ascending ramus is slender, high (*H* = 142.4 mm measured at the condyle level), and longer (L = 168.2 mm) than the p3–m3 series length (L = 149.3 mm). The angular process forms an ear-shaped, markedly extended large expansion, having a thick border on its lateral side (Fig. 2A, C). Externally, the large masseteric fossa is concave-convex in the dorsal–ventral direction (Fig. 2A, C).

In the right hemimandible (Fig. 2D-G), the dorsal border or incisura mandibular (area between the coronoid process and the condyle; Fig. 2C-D) is almost straight in lateral view but S-shaped in dorsal view (Fig. 2E). The area of the coronoid process is thick, and the border becomes thinner going backwards to the condyle (Fig. 2E). The anterior border of the ascending ramus is undulated (Fig. 2F), thicker than the dorsal border and shifted anteriorly (as in *Pyrotherium*), hiding the m3 in lateral view (Fig. 2D-E). Internally, just below the coronoid process, there is a longitudinal tuberosity for the *m. temporalis* (Fig. 2F). The condyle (better preserved in the right ramus) is an ovoid and low structure, well extended towards the internal side of the mandible (Fig. 2F-G); its transversal diameter is larger (55.3 mm) than the anteroposterior diameter (30.7 mm) and has a laterally convex surface (Fig. 2D-E).

On the medial side of the ascending ramus (better observed in the right hemimandibule), there is a large aperture posterolateral to the m3, which is interpreted


A
p3
p4
m1
inc. al
inc. al
B
C
inc. al
D
en
E
F
G
H
pa
*
*
inc. al
I
cor. pr
J
lbtb
cre
lbcd
lbtb
mtfd
cr
hpcd
prtd
mcd
cro
lbtb
lbtb
cro
pl-pa
cre
etcd
lgtb
mtcd
lgtb
dcd
lgtb
dcd
etfd
lgtb
m3
m2
m1
p4
p3

◂**Fig. 3** *Propyrotherium saxeum*. **A–J** LIEB-PV 3200: **A–C** symphysis preserving the left tusk-like incisor alveolus and part of the right ramus with p3–4 and tusk-like incisor alveolus in dorsal (**A**), ventral (**B**), and anterior (**C**) views; **D–G** fragment of left i2? in lateral (**D**), dorsal (**E**), anterior (**F**), and posterior (**G**) views; **H–J** left mandible with p3–m3 in anterior (**H**) and occlusal (**I**) views (**J**, schematic lineal drawing). Abbreviations: cor. pr, coronoid process; cr, cristid; cre, crenulations; cro, cristid obliqua; dcd, distal cingulid; en, enamel; etcd, entoconid; etfd, entolophid (=posterior lophid); hpcd, hypoconid; inc. al, incisor alveolus; lbcd, labial cingulid; lbtb, labial tubercle; lgtb, lingual tubercle; mcd, mesial cingulid; mtcd, metaconid; mtfd, metalophid (=anterior lophid); pl-pa, paralophid-paraconid; prtd, protoconid. *Indicates the narrowness of the mandibular bone in front of the p3, just where the anterior border of the symphysis and the tusk alveolus are placed. Arrow (in **D**, **E**) indicates anterior end of incisor. All scale bars represent 20 mm (**B**, **C**, **F–H**, not at scale)

as the anterior exit of the coronoid canal (Fig. 2D). The canal perforates the ascending ramus posterior to the m3, forming a short and oblique "bony bridge" between the horizontal and vertical rami of the mandible (Fig. 2B, D-E, G). The posterior exit of the coronoid canal opens just above the also large mandibular foramen, both being vertically communicated (Fig. 2G). In the medial view, the coronoid canal, its two exits, and the mandibular foramen are all close to each other and placed at a mid-distance between the coronoid process and the condyle (Fig. 2D). A coronoid canal is also observed in *Pyrotherium* (e.g., FMNH P 12,987) and in the Xenungulata *Carodnia* sp. and *Notoetayoa* sp. (Gelfo et al., 2008; Antoine et al. 2015). It was reported in many other groups of extinct and extant mammals such as proboscideans, sirenians, hyracoids, lagomorphs, xenarthrans, artiodactyls, and perissodactyls (see Ferretti and Debruyne 2011; Tabuce et al. 2012; Brocklehurst et al. 2016 and its respective references).

The symphysis is short, low, and narrow (Fig. 3A-C). Its anterior-most border is partially broken in the right mandibular ramus, but in the left ramus the close position of the border of the incisor alveoli (Fig. 3C) and the constriction of the dentary bone in front of p3 (see the asterisk in Fig. 3H) indicate that the anterior border of the symphysis should have been extended just a bit forward from the p3. The posterior border of the symphysis reaches the p4/m1 level (Fig. 3A) occupying an anteroposterior length of 38.9 mm, approximately (Fig. 3B). Anatomically, both mandibular rami of LIEB-PV 3200 diverge markedly backwards from the symphysis (Fig. 3A). This configuration implies a short distance in the anterior part of the symphysis to accommodate the external part of the tusk-like teeth (Fig. 3A, C and see below). The posterior border of the incisor alveoli extends to the m1 level (Fig. 3I), as in *Pyrotherium*, while in *Proticia*, the tusk-like incisor extends back, at least beneath the p4 (Patterson 1977).

Tusk-like tooth One fragment of a tusk-like tooth (Fig. 3D-G) was recovered together with the mandible LIEB-PV 3200, which fits very well into the partial alveolus of the left hemimandible (Fig. 3H-I). Here, with the available evidence, we cannot definitively infer its locus position. However, considering that *Pyrotherium* has two upper tusk-like teeth (I1–2) and only one pair of tusk-like teeth considered as the i2's (Loomis 1914; Billet et al. 2010), we suggest that the left lower tusk-like tooth of LIEB-PV 3200 could be the i2. This tooth (i2) is longitudinally curved (L = 97.8 mm) and slightly twisted laterally (Fig. 3D-E). Its anterior end (outer part) is nearly circular in contour (TD = 26.2 mm; Fig. 3F), while the most posterior end (inner part) is narrower, with a hollow base (16.9 mm × 19.6 mm; Fig. 3G). On the anterior end of the tooth, there are patches of enamel over the lateral sides that indicate the base of the crown of the incisor (the tip is lacking; Fig. 3D). Anatomically speaking (incisor into its alveolus), the twisting of this tooth allows it to diverge laterally, as in *Pyrotherium*. It would allow the incisor crown to diverge slightly from the alveolus, avoiding contact with the other incisor and accommodating both teeth in such a narrow symphysis (Fig. 3C). The i2 of LIEB-PV 3200 is similar in size and general aspect (e.g., curvature, lateral enamel) to the lower tusk-like tooth of MACN-A 10.929 (paralectotype of *Propyrotherium saxeum*; Ameghino 1901: Fig. 18). Comparatively, the lower incisors of *Propyrotherium* are narrower and shorter than in *Pyrotherium*, where despite also having a narrow symphysis, their incisors are enormous and much more developed externally (Gaudry 1909; Loomis 1914; Table 1).

Lower cheek teeth LIEB-PV 3200 is a young adult given by its practically unworn teeth, except the highly worn m1 (Fig. 3I-J; see below). The p3–m3 are bilophodont, bi-rooted, and longer than wide teeth, whose sizes increase from the p3 to m3 (Table 1). In the p3 and m3, the anterior and posterior lophids are transverse, nearly straight, and parallel to each other; in p4, in turn, the anterior lophid is a bit mesially concave, whereas in m1–m2 the lophids are divergent curves. The anterior lophid is labio-lingually narrower than the posterior lophid in p3–4; in m1–2, both lophids are nearly similar in transverse width, whereas in m3 the anterior lophid is wider than the posterior one. The distal cingulid is unquestionably present in p3–m3. It is a well-developed platform occupying all the distal face and becomes longer and better extended from p3 to m3. In turn, mesial cingulid is not observable in p4 and m3, whereas a very thin mesial cingulid is present in m1–2 (Fig. 3J). The anterior and posterior lophids are centrally connected by a longitudinal cristid, which extends from the mesial edge of the posterior lophid to the distal base of the anterior lophid. This cristid (cristid obliqua?) is thin in premolars and thicker in molars. A similar structure was noted in the p4 and m1

Table 1 Comparative measurements (in mm) for lower teeth of pyrotheres. D, diameters; L, length; aW, width anterior lophid; pW, width posterior lophid; *values taken from Kramarz and Bond (2014). Approximate measurements between parentheses (e.g., broken teeth)

Specimens	i2?		p3			p4			m1			m2			m1 or m2		m3		
Dimensions	D	L	L	aW	pW	L	aW	pW	L	aW	pW	L	aW	pW	L	aW	L	aW	pW
LIEB-PV 3200 left			(29.2)	(17.3)	(19.1)	26.5	(19.8)	(22.1)		28.1	(22.4)	22.8	31.7	23.9	(26.7)			32.8	25.1	23.5
LIEB-PV 3200 right	24.7×23.9	(150)			19.6	26.5	(19.1)	(20.7)												
LIEB-PV 3201										29.5	23.7	23.2								23.0
MACN-A 10.929 (paralectotype)	23×18	140				28.0		25.1												
MLP 55-III-10-1b													33.9		27.2			31.4	36.3	
MLP 61-IV-17–1-2*																		42.5	36.0	
AMNH FM 29,392																		35.5	30	
AMNH FM 29,393*													35		29					
AMNH FM 29,394																				
Griphodon					16	29.5	19.0	21.5		32.2	25.8	25.5								
Proticia			38.1	23.4	31.6	35.0	34.4	32.9		>26.0	29.2	26.8								
Carolozittelia																23.6	18.3	(27.3)		
Pyrotherium (MACN-A 52-601b)	58.4×40.4		51.6	32.1		48.3	43.7			46.9	53.2		51.4	62.7				61.5	68.2	

of *Griphodon* by Patterson (1942:4), who described this as a swelling on the external half of the anterior slope of the metalophid. In the m1 of LIEB-PV 3200, a shorter but well-formed longitudinal cristid runs centrally from the distal cingulid to the distal edge of the posterior lophid, forming two deep basins towards the labial and lingual sides from this cristid (labelled as "cr" on Fig. 3J). The labial basin is wider than the lingual one, which is almost closed. In the m2–3, in turn, there is a conspicuous tubercle in contact with both the distal cingulid and the posterior lophid, which with high wear could probably form a cristid as observed in m1. These features (tubercle and crista) are not observed in the p3–4. In the p4–m3, there are two low and conic tubercles (interlobular tubercles sensu Ameghino 1897) located labially and lingually at the base of the valley between anterior and posterior lophids (labial and lingual tubercles; Fig. 3HJ). In p3, the labial cuspid is the only one observed, having its lingual face partially broken. Regarding these tubercles, two peculiar characteristics should be noted in LIEB-PV 3200: (1) the tubercles increase in size from p4 to m3, and (2) the labial tubercle is larger than the lingual one, a useful feature to distinguish highly worn isolated teeth (see m1 below). A small labial tubercle was described for the lower cheek teeth of *Pyrotherium romeroi* and also in the p4 and m1 of *Pyrotherium macfaddeni* (cuspule sensu Shockey and Anaya 2004). Concerning the labial cingulid, it does not properly form a well-developed platform along the crown. Indeed, in LIEB-PV 3200 there is a very short labial cingulid joining the labial tubercle with the anterior lophid of the m1–2, and a thin labial cingulid is variable observable between distal cingulid and posterior lophid of the m1–3 (see m1 LIEB-PV 3201). In turn, the presence of labial cingulid could not be confirmed in the p3–4 because they are broken in this area.

Both p3s of LIEB-PV 3200 (Fig. 3I-J) have partially broken their anterior lophid and crown. In the left p3, the metalophid is more worn than the entolophid. An unworn small conid is observed low in the middle of the mesial face. It could be interpreted as a trace of paraconid or as a remnant of mesial cingulid but considering that the latter is absent in p4 (see below), we opt to consider this structure as part of the paraconid/paralophid (Fig. 3J). The presence of this structure differentiates the p3 from the p4 and molars. A prominent mesial cuspid in the p4 of *Griphodon* was described undoubtedly as the paraconid, which is possibly present in the p3 as well (Patterson 1942). In *Pyrotherium*, the p3 is well distinguished from the p4, being a triangular and longer tooth with a robust mesial cuspid, while in LIEB-PV 3200 the p3 is rectangular in contour and quite similar to the p4 (except by having a mesial cuspid), with a wider valley separating the lophids.

The p4 of LIEB-PV 3200 (Fig. 3I-J) is a molariform tooth, being similar to the molars by lacking paralophid

and paraconid. The p4 shows relatively more wear than the m2 (see below). Its lophids display distally inclined occlusal wear facets, the metalophid being more worn than the entolophid. In addition, asymmetrical wear is observed in the entolophid, whose labial side is more worn than the lingual side. The labial tubercle closing the central valley is more worn than the lingual tubercle. The p4 of LIEB-PV 3200 is comparable in size and morphology to the p4 MACN-A 10.929 (paralectotype of *Propyrotherium saxeum*; Fig. 4A, B; Table 1). Both are bilophodont and longer than wide teeth, with an anterior lophid labiolingually narrower than the posterior one, and having a well-developed distal cingulid, a thinner labial cingulid, and labial and lingual small tubercles closing the central valley (in MACN-A 10.929 the labial tubercle is barely distinguished, while the lingual one was likely present but eroded by wear). However, a wider valley separating the distal cingulid from the posterior lophid and a distinct central cristid joining anterior and posterior lophids differentiate LIEB-PV 3200 from MACN-A 10.929. In the latter specimen, the distal cingulid is practically in contact with the distal wall of the posterior lophid, and the central cristid is barely noticeable. These differences (e.g., narrow lophid-cingulid contact and barely noticeable central

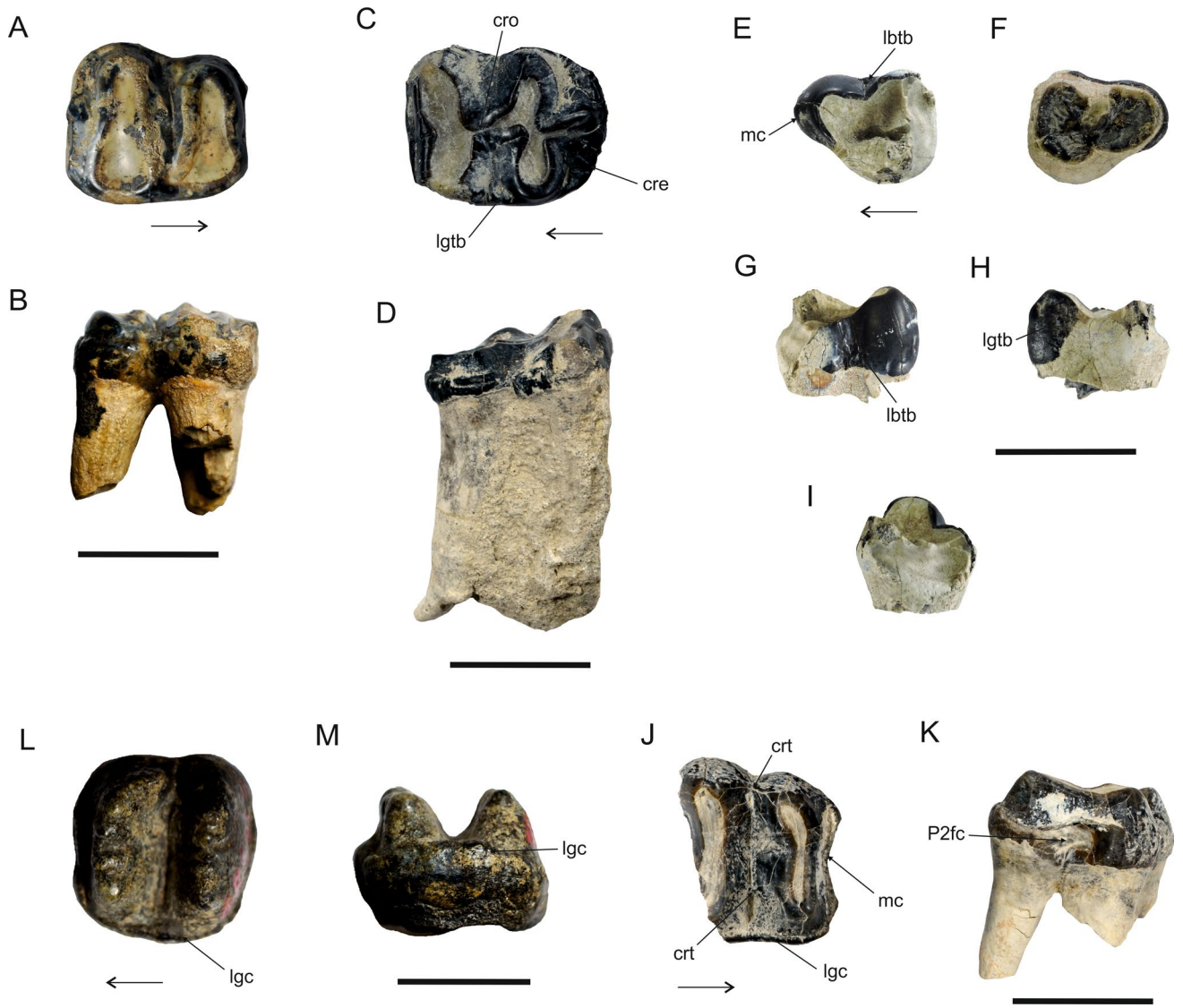

Fig. 4 *Propyrotherium saxeum*. **A**-**B** MACN-A 10.929 (paralectotype), left lower cheek tooth (p4?), in occlusal and labial views. **C–D**, LIEB-PV 3201, right m1 in occlusal and labial views. **E–I** LIEB-PV 3208, left P2, in occlusal (**E**), ventral (**F**), labial (**G**), lingual (**H**), and distal (**I**) views. **J–K** LIEB-PV 3202, right P3, in occlusal and mesial views. **L–M** MACN-A 10.929 (lectotype), left P4, in occlusal and lingual views. Abbreviations: cre, crenulations; cro, cristid obliqua; crt, crest; lgc, lingual cingulum; lbtb, labial tubercule; lgtb, lingual tubercle; mc, mesial cingulum; P2fc, facet for P2. Arrows show mesial side. All scale bars represent 20 mm

cristid) could be explained by intraspecific variation between p4 MACN-A 10.929 and that of LIEB-PV 3200.

The m1 of LIEB-PV 3200 is smaller and much more worn than the m2 and closer in size to the p4 (Table 1). It has a low crown and a well-exposed dentine area on the lophids and the distal cingulid. The wear in m1 reveals that the central cristid forms a continuous occlusal surface with the metalophid and entolophid, which are nearly at the same level as the labial and lingual cuspids (Fig. 3I-J). A similar wear degree is observed on the occlusal surface of the cristid joining the posterior lophid with the distal cingulid, and the lingual half of the distal cingulid. The occlusal surfaces of the lophids are differentially erased, the lingual side of the entolophid being more worn, which is traduced in a wider and deeper surface than that of the metalophid.

The m2 of LIEB-PV 3200 is similar to the m1 but differs from it in being a larger tooth (Table 1). The posterior lophid is wider transversely than the anterior one, a difference more marked than in the m1 where the width of lophids are almost identical (Fig. 3I, J; Table 1). The metalophid shows a slightly erased occlusal surface, as in the p3, while the entolophid and the distal cingulid have no trace of wearing, differing from the condition in p4.

The m3 of LIEB-PV 3200 seems to be a recently erupted tooth, having no worn occlusal surfaces (Fig. 3I-J). It differs from the m1–2 in having a posterior lophid transversely narrower than the anterior lophid and is characterized by having a better-developed distal cingulid with a wider longitudinal cristid. In the m3, the entolophid and the distal cingulid show crenulated surfaces, versus smooth surfaces on the premolars and m1 and softer crenulations in m2 (Fig. 3I-J). The metaconid and entoconid are better developed, anteroposteriorly extended, and wider than in m2 and evidently the m1. The m3 has the metalophid higher than the entolophid, which is different than the m2 where both lophids are at the same height. This difference in height leads to differentiated wear between the lophids (see below). Based on the stage of wear on the teeth of LIEB-PV 3200, we can deduce that the m3 is the last tooth to erupt, even after premolars. A similar condition is observed in *Pyrotherium* (e.g., FMNH P 12,987). This trait, the p4 erupting before m3, was also documented by other South American Paleogene ungulates, such as *Notostylops*, *Henricosbornia*, and *Notopithecus* (see Vera and Cerdeño 2014; Vera 2016).

Compared to the teeth of LIEB-PV 3200, the isolated right lower molar LIEB-PV 3201 (Fig. 4C, D) has an approximate size and similar wear pattern to that of the m1 in addition to similar widths of both lophids, unlike what occurs in m2 where the posterior lophid is wider than the anterior lophid (Table 1). LIEB-PV 3201 displays less wear than the m1 LIEB-PV 3200, allowing for the observation of the crenulated border on its unworn distal cingulid and the labial position of the central cristid with respect to the posterior cristid (Fig. 4C). LIEB-PV 3201 differs from the m1 LIEB-PV 3200 in having only a lingual tubercle (versus labial and lingual tubercles present in LIEB-PV 3200) and a thin labial cingulid around the posterior lophid, indicating variability in these features.

Among pyrotheres, mandible and lower cheek teeth are known in *Pyrotherium* spp., *Carolozittelia*, *Griphodon*, and *Proticia*. Comparatively, LIEB-PV 3200 is much smaller than *Pyrotherium* (~45% smaller using mandible and molar lengths; Table 1). *Propyrotherium* and *Pyrotherium* share a longer than high ascending ramus of the mandible, but in *Pyrotherium*, the ascending ramus does not laterally hide the m3, has a concave incisura mandibular, no expanded angular process, and a relatively higher mandibular condyle. *Griphodon* shares a comparable size (using teeth lengths; Table 1) and a distinct paraconid in p3 with LIEB-PV 3200. However, in *Griphodon*, the p3−4 are not true bilophodont teeth, having a labial cristid running from the posterior lophid to the anterior lophid and a distinct paraconid in both premolars. In addition, the m1 of *Griphodon* has a clearly bilobed contour, non-divergent lophids and lacks central cristid and labial and lingual cuspids. *Proticia* is much larger than LIEB-PV 3200 and completely differs from it in having bunodont teeth, a m1 smaller than premolars, and a different relationship between the width of the anterior/posterior lophids in p4 and m1. A lower canine was attributed to *Carolozittelia tapiroides* (Ameghino 1901: Fig. 16) as a defense-tooth with limited growth and much smaller size than the incisor MACN-A 10.929 of *Propyrotherium saxeum* with continuous growth (Ameghino 1906). *Carolozittelia* also differs from *Propyrotherium* primarily by having smaller lower molars, which present oblique lophids, labial, and lingual cristids running obliquely from the entolophid to the metalophid, straighter and non-crenulated lophids, smaller distal cingulid, distinct mesial cingulid, and lacking labial and lingual tubercles in the central valley.

Upper cheek teeth Until presently, no upper canines nor P1 were reported for *Propyrotherium saxeum*, except fragments of a probable upper tusk (see Simpson 1967). Among the pyrothere teeth recovered in Cañadón Pelado, only two specimens, LIEB-PV 3202 and LIEB-PV 3208 are positively identified as upper teeth (Fig. 4E-K). Compared with the known pyrotheres, LIEB-PV 3202 and LIEB-PV 3208 resemble the P3 and P2, respectively, of *Pyrotherium romeroi* (Gaudry, 1909). The left P2 LIEB-PV 3208 (Fig. 4E-I) and the right P3 LIEB-PV 3202 Fig. 4J-K) could represent opposite sides of the same individual, but their different state of wear and enamel coloration do not allow for the confirmation of this supposition.

The P2 LIEB-PV 3208 has a triangular contour, is longer than it is wide (Table 2), with a lobed perimeter (Fig. 4E).

Table 2 Comparative measurements (in mm) for upper teeth of pyrotheres. L, length; W, width; aW, width anterior lophid; pW, width posterior lophid; *values taken from Kramarz and Bond (2014)

Specimens Dimensions	P2		P3			P4		M1		M2		M1 or M2		M3	
	L	W	L	aW	pW	L	W	L	W	L	W	L	W	L	W
LIEB-PV 3208	21.6	16.5													
LIEB-PV 3202			> 24.8	25.6	> 27.3										
MACN-A 10.929 (lectotype)						30.0	30.1								
AMNH FM 29,391*			29.5		28.0										
MLP 55-III-10-1a*												32.0	31.7		
MLP 55-III-28-1a*												30.7	34.8		
AMNH sin número (O3)*														42.0	35.0
MACN-A 52–297													34.0		
Baguatherium		20.5	32.7	33.1											
Carolozittelia										23.4	24.1			24.3	24.6
Pyrotherium	42.6	31.2	44.9	49.6		51.9	59.7	52.9	64.1	65.6	77.6			80.1	83.5

Three coalescent blunt cusps give this configuration: a robust mesial cusp and two distal cusps on the labial and lingual sides. A shallow lingual entrance and a deeper labial sulcus delimit the mesial cone from the two distal cones. The enamel is mainly concentrated around the mesial lobe and the labial face (Fig. 4G) but is absent or reduced on the lingual and distal faces of the distal lobes (Fig. 4H). There are two tiny tubercles, one in the labial sulcus at the base of the crown (Fig. 4E, G) and the other on the enamel layer on the anterolingual side (Fig. 4H). A bulge of enamel forms a small mesial cingulum (Fig. 4E), differing from the well-defined shelf in *Pyrotherium*. The occlusal surface is irregular and deeply excavated, having an irregular pit of dentine in the center (Fig. 4E). This pit or central fossette has no enamel inside. The posterior-most border of the occlusal surface is a thin crest transversely oriented (Fig. 4E, I). Beyond this crest is a downwardly inclined area on the distal face. This sloping area is in fact a concave-convex surface, transversely oriented and lacking enamel (Fig. 4I). By its characteristics, we interpret it as a contact surface for the anterior loph of the P3, but no certain evidence is available to confirm that supposition. The P2 is a two-rooted tooth (Fig. 4F), differing completely in shape and size from the three-rooted and bilophodont premolars (P3 or P4, see below; Table 2). These marked differences were also noted between the P2 and P3 of *Pyrotherium* spp. (Gaudry 1909; Shockey and Anaya, 2004) and *Baguatherium* (Salas et al. 2006). Comparatively, a triangular-shaped and longer than wide P2 is present as well in *Pyrotherium* spp. and *Baguatherium*, but a three-rooted P2 with a well-developed mesial cingulum is present in the former (e.g., *P. macfaddeni*, Shockey and Anaya, 2004), whereas a small anterior conule is present in the bi-rooted P2 of *Baguatherium* (Salas et al., 2006).

The P3 LIEB-PV 3202 (Fig. 4J, K) is broken in the distolingual corner, but it has a square-shaped contour (Fig. 4J), which is a characteristic of the upper teeth of pyrotheres (e.g., *Pyrotherium*, *Baguatherium*, and *Colombitherium*), differing from the longer than wide relationship typical of lower teeth (e.g., the mandible LIEB-PV 3200). It has three roots (one lingual and two labial; Fig. 4K), as Kramarz and Bond (2014) noted for upper teeth of *P. saxeum*, but differing from the bi-rooted P2 here described (see above). LIEB-PV 3202 is a bilophodont tooth. The anterior loph is labiolingually narrower and a bit higher than the posterior loph (Fig. 4J; Table 2). In addition, the anterior loph bears a narrower protoloph that is slightly mesially inclined, while the posterior loph has a distally inclined metaloph. The paracone, metacone, and hypocone are distally curved, differing from the protocone. Thus, the protoloph insinuates an inverted L-shape, while the metaloph is curved (Fig. 4J). The lingual cingulum is thin but clearly distinct and moderately high; it closes the central valley and extends around the protocone to connect with the mesial cingulum (Fig. 4J). The mesial cingulum is as thin as the lingual cingulum but a bit higher (Fig. 4K). In the mesial face, there is a concave surface for contact with the P2 (Fig. 4K). The central valley is deep, narrow, and straight. Labially, a very short and thin crest that joins the paracone and metacone walls limits it. A similar thin and short crest, more lingually placed, closes the central valley. Between this crest and the lingual cingulum, a deep and elongated pit is formed (Fig. 4J).

The P3 LIEB-PV 3202 shares similar features with the P4 MACN-A 10.929 (lectotype of *Propyrotherium saxeum*; Fig. 4L, M), such as the presence of mesial and lingual cingula and a distally curved protocone. However, the P3 LIEB-PV 3202 differs from the P4 MACN-A 10.929 in having the anterior loph narrower than the posterior loph (crenulated and almost similar widths in P4 MACN-A 10.929) and a mesially convex posterior loph (versus straighter posterior loph in MACN-A 10.929). Following the condition observed

in the lower premolars of LIEB-PV 3200, where the anterior lophid is narrower than the posterior one, and this difference is greater in p3 than in p4, a similar relationship occurs when comparing MACN-A 10.929 and LIEB-PV 3202. Thus, in MACN-A 10.929, the difference in width between the anterior and posterior lophs is lesser than in the P3 LIEB-PV 3202, which supports the attribution of the lectotype MACN-A 10.929 as a left P4, as was previously inferred (Simpson 1967; Kramarz and Bond 2014). This difference in shape between the P3 and P4 is also seen in *Pyrotherium* spp. and *Colombitherium* (Billet et al. 2010: Fig. 1). Comparatively, the P3 of *Pyrotherium* is a pi-shaped and four-rooted tooth, with labial and lingual cingula, lingual tubercle in the valley, and lingual crenulations. In *Baguatherium*, the P3 also has a conspicuous pi-shaped appearance as *Pyrotherium* but shares the presence of three roots and a lingual cingulum with *Propyrotherium.*

Until presently, upper molars were not identified among the sample from the Cañadón Pelado locality. However, Kramarz and Bond (2014: Fig. 2) described and figured as *P. saxeum* a right M1 or M2 (MLP 55-III-10-1a), a left M1 or M2 (MLP 55-IX-28-1a), and a right M3 (AMNH unnumbered labelled as "O3"). Despite not being homologous pieces, these molars are comparable to the P3 of Cañadón Pelado. MLP 55-III-10-1a is similar to LIEB-PV 3202 in the configuration of the anterior loph and the mesial and lingual cingula, but in the molar MLP 55-III-10-1a, the posterior loph is distally more curved and seems to be narrower than in P3 LIEB-PV 3202. At the same time, MLP 55-III-10-1a clearly differs from the M3 AMNH "O3," which has a curved posterior loph. As observed by Kramarz and Bond (2014), the curvature of the posterior loph gradually increases from premolars, where it is subtle, to being more evident in molars and being greatly curved in the M3. In *Pyrotherium*, upper molars also have curved lophs, but not so extremely curved as the posterior loph in the M3 of *Propyrotherium*.

Discussion

Propyrotherium saxeum was described based on a few isolated teeth (MACN-A 10.929, a lower tusk-like tooth, and left P4 and p4) and considered the unique member of Pyrotheria from the Mustersan SALMA of Patagonia, Argentina (Ameghino 1901, 1904). Since then, only a small number of other specimens based on isolated teeth (upper and lower check teeth) were reported for this taxon (Simpson 1967; Kramarz and Bond 2014).

Here, an almost complete mandible (preserving symphysis, left ramus, and part of the right ramus) with an associated lower tusk-like tooth (LIEB-PV 3200), as well as a left P2 (LIEB-PV 3208), a right P3 (LIEB-PV 3202), and other isolated lower molar (LIEB-PV 3201) from the Sarmiento Formation outcrops of the Cañadón Pelado locality (western Chubut Province) are recognized as *Propyrotherium saxeum*. We based our identification mainly on the close morphometric similitude between the new specimens LIEB-PV 3200 and LIEBPV 3202 and the type specimens of *P. saxeum* (MACN-A 10.929) but also compared to the other recently attributed specimens (Kramarz and Bond 2014).

The mandible of *Propyrotherium saxeum* is peculiar among pyrotheres due to several features. On the one hand, the ascending ramus is posteriorly well expanded (i.e., the area including the angular process); its anterior border laterally hides the m3; and dorsally, the incisura mandibular is nearly straight between the coronoid process and the condyle. The anterior edge of the mandibular ramus is shifted anteriorly, partly hiding the m3 in lateral view as was also described for the Xenungulata *Carodnia* (see Antoine et al. 2015). On the other hand, the presence of a coronoid canal is reported for the first time in *Propyrotherium*. This feature is also shared not only with *Pyrotherium* and with some Xenungulata (e.g., *Cardonia* and *Notoetayoa*; Gelfo et al., 2008; Antoine et al. 2015), among SANUs, but also with several other groups of extinct and extant mammals (see Ferretti and Debruyne 2011; Tabuce et al. 2012; Brocklehurst et al. 2016 and references in there).

Concerning the dentition of *Propyrotherium saxeum*, we report a fragment of the left tusk-like tooth, i2?, which fits into the incisor alveolus of the mandible of LIEB-PV 3200. Knowing the number of lower anterior teeth (incisors and canines) present in *Propyrotherium* is a difficult issue considering the state of the preservation of the symphysis LIEB-PV 3200. However, anatomically, both mandibular rami of LIEB-PV 3200 markedly diverge backwards, and the symphysis is very short and narrow, which implies a short enough distance in the anterior part of the symphysis to accommodate no more than a pair of tusk-like teeth (Fig. 3A, C). If extra lower teeth (other incisors and/or canines) were present, they would be rudimentary teeth (no space left for them in front of the symphysis between the two large alveolus, as was also observed in *Pyrotherium* by Loomis (1914). In *Pyrotherium*, for example, there are two pairs of upper tusk-like incisors (I1−I2) and only one pair of lower tusk-like incisors (i2?), while the i1, i3, and C/c are lacking (Loomis 1914; Billet et al. 2010). Unfortunately, the presence of upper incisors, canines, and P1 cannot be established with the available evidence.

We confirm the presence of P2, as proposed by Kramarz and Bond (2014), who inferred the formula P2–M3/p2–m3 for *Propyrotherium saxeum*. However, concerning the putative presence of the p2 tooth as was proposed by several authors (Simpson 1967; Kramarz and Bond 2014), it should be discarded. In the left mandible LIEB-PV 3200, the dentary bone becomes markedly thinner in front of the p3 (see

* in Fig. 3H), precisely where the tusk alveolus is placed (Fig. 3C, H). That is, the thinness and the constriction of the bone in front of p3 would not accommodate other teeth, neither as a p2 nor a p1, assuming the p3–m3 formula for the lower cheek teeth series of LIEB-PV 3200. A similar condition (p2 absent) was described for *Pyrotherium* (Ameghino 1897; Gaudry 1909) and indirectly inferred for *Baguatherium* (Salas et al. 2006). This formula (P2−M3/p3−m3) is shared with *Pyrotherium*, but it cannot be fully corroborated in any other pyrotheres, although the P2 is also present in *Baguatherium* and *Colombitherium*.

The new specimens from Cañadón Pelado allow us to improve the knowledge of *Propyrotherium saxeum*, differentiating it from other pyrotheres. *Propyrotherium* is characterized by its peculiar mandible, which laterally hides the m3 (as in the Xenungulate *Carodnia*) and has a straight incisura mandibular and a well-expanded angular process. *Propyrotherium* is much smaller (~45%) than *Pyrotherium* (e.g., *P. romeroi*) and differs from it in having an i2? that is narrower, shorter, and less developed externally; a p3 bilophodont, rectangular and quite similar to the p4; a two-rooted P2 and a three-rooted P3; mesial cingulum less-developed; and a greatly curved posterior loph in M3. *Propyrotherium* has a comparable size (based on teeth lengths) to *Griphodon* but differs from it, and also from *Carolozittelia* and *Proticia* in having a longitudinal cristid between lophids, labial, and mesial tubercles in the central valley, and crenulations in lophids and cingulids. *Propyrotherium* has fully lophodont cheek teeth, differing from *Proticia*.

The new specimens from Cañadón Pelado also allow us to re-examine isolated teeth from several fossil sites in Chubut Province previously referred to as this taxon (Simpson 1967; Kramarz and Bond 2014). Among the lower molars attributed to *P. saxeum*, AMNH FM 29,394 and MLP 55-III-10-1b were both considered as m1 or m2 of *P. saxeum* (see Simpson 1967; Kramarz and Bond 2014). These molars are unworn and similar to each other. They have the anterior lophid narrower transversally than the posterior lophid, a feature that distinguishes the m2 from m1 in LIEB-PV 3200. In fact, AMNH FM 29,394 and MLP 55-III-10-1b have comparable dimensions to the m2 of LIEB-PV 3200 (Table 1), although some features differentiate them from the molars of LIEB-PV 3200, such as the absence of labial and lingual tubercles, a mesially concave posterior lophid (versus convex), and no well-defined central cristid. Although the available sample of *Propyrotherium* is still small, these differences may be related to intra-specific variability, considering both AMNH FM 29,394 and MLP 55-III-10-1b as m2's of *P. saxeum*.

The specimen AMNH FM 29,393, figured as a right m3 by Kramarz and Bond (2014), matches well with the m3 of LIEB-PV 3200, although it is very worn and somewhat larger (Fig. 3I, J; Table 1). Both teeth share an anterior lophid wider than the posterior one, a central cristid, and a well-expanded distal cingulid (or heel). In AMNH FM 29,393, the central cristid is nearly touching the anterior lophid, given by the high wear. In LIEB-PV 3200, the labial and lingual tubercles are conspicuous, but they are absent on AMNH FM 29,393. Likewise, this apparent lack of labial and lingual tubercles in AMNH FM 29,393 could be indicative of intraspecific variation, as was noted for the m2 AMNH FM 29,394 and MLP 55-III-10-1b (see above). The variable presence of labial and lingual tubercles in the central valley of lower molars was also reported in the *Pyrotherium* species (Cerdeño and Vera 2017).

The specimen AMNH FM 29,392 was identified as a M3 or m3 of *P. saxeum* by Simpson (1967), but as a right unworn m3? of a Pyrotheriidae sp. 2 by Kramarz and Bond (2014) because they consider that this tooth exceeds the probable intraspecific variation of *P. saxeum*. AMNH FM 29,392 is characterized by having an anterior lophid labiolingually wider than the posterior lophid, a condition described for the m3 of LIEB-PV 3200 (see above; Fig. 3I, J). Moreover, the m3 AMNH FM 29,392 has a similar width to the m3 of LIEB-PV 3200 (Table 1), sharing labial and lingual tubercles closing the central valley and a well-expanded distal cingulid with a central cristid. However, AMNH FM 29,392 is longer than LIEB-PV 3200 (Table 1) and lacks well-defined central cristid joining lophids. Although these features can be explained by intraspecific variation, as in the other cases, we consider that AMNH FM 29,392 should be considered at least co-generic with LIEB-PV 3200.

Regarding isolated upper teeth, AMNH FM 29,391 was interpreted as a probable upper molar of *P. ?saxeum* by Simpson (1967) and as likely a right P3 or deciduous premolar of *P. saxeum* by Kramarz and Bond (2014). It shares with the P3 LIEB-PV 3202 a L-shaped protoloph and well-developed mesial and lingual cingula but differs from it by the presence of labial and lingual tubercles closing the central valley (lacking in P3 LIEB-PV 3202) and being a bit longer than wide tooth (Table 2). On the one hand, the presence of tubercles in upper premolars seems to be a variable feature in the upper cheek teeth of *Propyrotherium*, such is observable in other specimens (e.g., absent in MLP 55-III-10-1a; the presence of a labial tubercle in AMNH "O3") referred to *P. saxeum* (Kramarz and Bond, 2014). On the other hand, the longer than wide condition of AMNH FM 29,391 is also observable in the DP3 of *Pyrotherium* (Gaudry, 1909); thus, it seems to be a characteristic of deciduous dentition as Kramarz and Bond (2014) proposed for AMNH FM 29,391, although more evidence is needed to confirm this hypothesis.

Phylogenetic relationships and cladistics analysis

Presently, the phylogenetic relationships of Pyrotheria have no overwhelming consensus, nor do the definitions of its groups Pyrotheriidae and Colombitheriidae. In one regard, Ameghino (1894) defined both Pyrotheria (as a suborder at that time) and the family Pyrotheriidae based on the characteristics of the skull and limb bones (e.g., astragalus and femur) of *Pyrotherium*. Among other features, Ameghino (1894) described Pyrotheria and Pyrotheriidae as having a pair of forwardly directed upper and lower tusk-like incisors, quadrangular, or rectangular upper and lower premolars (P2−4/p3−4), and molars (M1−3/m1−3), and lacking canines. In 1901, Ameghino included *Propyrotherium* into Pyrotheriidae, considering it as the direct ancestor of *Pyrotherium*, and defined the family Carolozittelidae to include, among others, the genus *Carolozittelia*, remarking they are the ancestors of Pyrotheriidae. Moreover, Ameghino (1901, 1906) related the pyrotheres to the proboscideans based on a series of changes he observed along the pyrotheres evolutionary line, from the Casamayoran *Carolozittelia* to the Deseadan *Pyrotherium*: (1) reduction in the number of molars; (2) gradual size increase of cheek teeth (e.g., in *Propyrotherium*) to molars relatively much larger than the premolars (e.g., in *Pyrotherium*); and (3) an increase in body size accompanied by tusk enlargement, from a tapir-like body size with very small and limited growing tusk (e.g., *Carolozittelia*) to larger body size with longer and ever-growing tusks (*Propyrotherium* and *Pyrotherium*). Later, Pyrotheria and Xenungulata have been proposed to be closely related to North American uintatheres (Dinocerata; Lucas 1986), while Patterson (1977) noted many resemblances between the auditory regions of *Pyrotherium* and Notoungulata. This latter hypothesis was subsequently re-established in a phylogenetic analysis by Billet et al. (2010), who noted resemblances between the anterior dentitions of *Pyrotherium* (Pyrotheria) and *Notostylops* (Notoungulata). Similar results were obtained by de Muizon et al. (2015: Fig. 121), whose constrained analysis supports the hypothesis of pyrotherian affinities with xenungulates, which were recovered as a natural group and sister to the notoungulates.

Concerning families of Pyrotheria, Carolozittelidae as a group, since its original proposition by Ameghino (1901), has been overlooked over the years. This group was no longer considered in the literature (e.g., Gaudry 1909; Scott 1913; Loomis 1914) until it was formally included (but without further discussion) into Pyrotheriidae, grouping *Carolozittelia*, *Propyrotherium*, *Griphodon*, and *Pyrotherium* (Simpson, 1945). However, Paula Couto (1952) pointed out the distinctiveness of *Carolozittelia* from the other pyrotheres, suggesting it could belong to the Xenungulata due to certain resemblances to *Carodnia* (e.g., bilophodont M1−2/m1−2), although without enough evidence. Following this idea, Simpson (1967) regarded both *Carolozittelia* and *Griphodon* as incertae sedis, probably pyrotheres, but perhaps xenungulates, considering only *Pyrotherium* and *Propyrotherium* into Pyrotheriidae. In the words of Simpson (1967: 238), the differences between *Carolozittelia* and *Propyrotherium* are undoubtedly greater than between most reasonably established ancestral-descendent Casamayoran and Mustersan genera (or species), and *Propyrotherium* is distinctly closer to Deseadan *Pyrotherium* than to Casamayoran *Carolozittelia*. Shortly after, Hoffstetter (1970) erected the family Colombitheriidae to include *Colombitherium tolimense*, whereas Patterson (1977) included *Proticia venezuelensis* as well. More recently, Salas et al. (2006) performed the first phylogenetic analysis of pyrotheres, in which Pyrotheriidae showed a well-supported clade including all taxa more closely related to *Pyrotherium* than to *Colombitherium* and *Proticia*. Although these authors indicated remarkable differences between *Carolozittelia* and *Baguatherium* and other pyrotheres, they retained *Carolozittelia* in the clade Pyrotheriidae (plus *Propyrotherium*, *Griphodon*, *Baguatherium*, and *Pyrotherium*), which is characterized by derived masticatory anatomy (lophodont teeth with oblique wear facets). However, Salas et al. (2006)'s analysis failed to support Colombitheriidae (*Proticia* + *Colombitherium*), suggesting it is paraphyletic. According to these authors, the Oligocene pyrotheres (*Baguatherium* and *Pyrotherium*) characterize by maxillary tooth series that tend to converge anteriorly, a wide molariform area enclosing a narrow palate, high and inclined lophs/lophids, oblique and almost flat wear facets, a narrow predental region of the maxilla, a maxillary dental formula of P2−M3, retracted nares, and the root of the zygomatic arch located at the level of P4 and M1. Currently, doubts exist concerning the inclusion of *Carolozittelia* in Pyrotheriidae, as well as considering *Proticia* and *Colombitherium* in Pyrotheria (Sánchez-Villagra et al. 2000; Billet et al. 2010; Croft et al. 2020).

Our cladistics analysis yielded two most parsimonious trees (TBR = 46 steps; consistency index = 0.72; retention index = 0.62). The only difference between these topologies is the iterative position of *Baguatherium*. In one of them, *Baguatherium* forms a clade with *Pyrotherium* sharing a non-ambiguous synapomorphy (3^1: pi-shaped P3–4). In the other topology, *Baguatherium* groups with *Propyrotherium* and shares a synapomorphy (28^0: bi-rooted P2). The consensus topology (Fig. 5), in consequence, groups *Propyrotherium*, *Baguatherium*, and *Pyrotherium* in an unresolved clade (node a, Fig. 5), which is supported by a synapomorphy: paraconid lacking in p4 (7^1), although this feature is unknown in *Baguatherium*. *Griphodon* appears as the sister taxon of the group *Propyrotherium-Baguatherium-Pyrotherium* (node b, Fig. 5), which is well supported by four synapomorphies: unequally developed mesial and distal cingulids (6^1), anterior lophid narrower than or similar to the

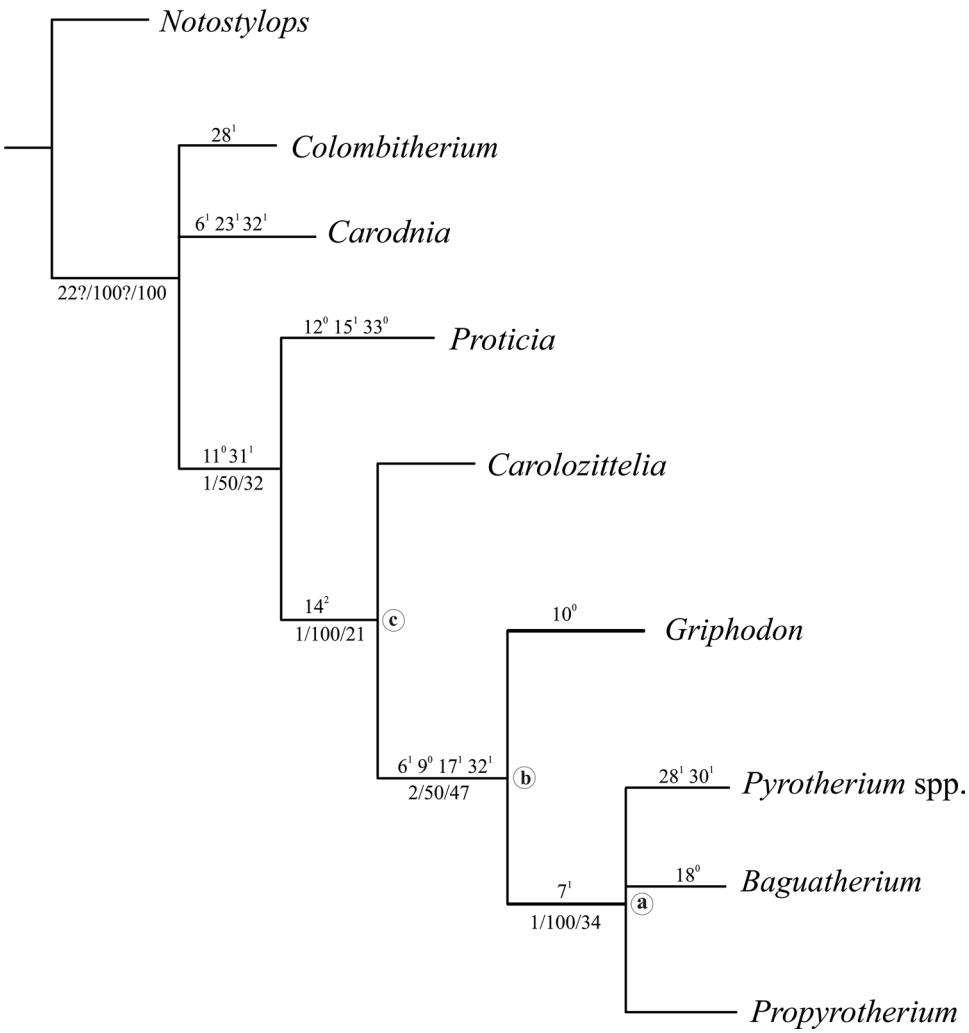

Fig. 5 The consensus tree (TBR = 46; CI = 0.72; RI = 0.62) obtained from the two most parsimonious trees yielded from the cladistics analysis. Synapomorphies are shown above rami, while support values and nodal support appear below rami. Letters a, b, and c indicate nodes, which are explained in the text

posterior one in the lower molars (9^0), presence of denticles or crenulations on loph/lophids (17^1), and loph/lophid height greater than length (32^1).

Analyzing the topology obtained, the position of *Propyrotherium* being more related with *Pyrotherium* and *Baguatherium* clearly differs from previous hypotheses, where *Propyrotherium* appears as an early diverging taxon of *Baguatherium-Griphodon-Pyrotherium* or forming a polytomy with all of them (Salas et al. 2006; Kramarz and Bond 2014). Furthermore, concerning the most recent analysis of Kramarz and Bond (2014), our analysis adds a new synapomorphy to the clade, including *Griphodon-Pyrotherium-Baguatherium-Propyrotherium* (node b; Fig. 5).

In addition, our results do not support the ideas conceived by Patterson (1942) concerning similarities between *Griphodon peruvianus* and *Propyrotherium saxeum*. According to Patterson (1942), *Griphodon peruvianus* is more similar, although slightly more advanced, to *Propyrotherium saxeum* than other pyrotheres. Based on that, this author proposed that the '*Griphodon* fauna' might fill the gap existing between the Mustersan and Deseadan SALMAS. However, the new specimens demonstrate that *Propyrotherium* displays more advanced features than *Griphodon*, mainly in the lower premolars.

Regarding *Carolozittelia*, it appears to be a sister taxon of the most inclusive group (*Griphodon* (*Pyrotherium*, *Baguatherium*, *Propyrotherium*)). This clade (node c, Fig. 5) represents the Pyrotheriidae, following previous authors (Salas et al. 2006; Kramarz and Bond 2014), which is supported by a synapomorphy, the bilophodont upper and lower cheek teeth (14^2, unequivocal). However, Kramarz and Bond (2014) obtained two other synapomorphies, in addition to the bilophodoncy condition, supporting Pyrotheriidae. These characteristics (see characters 6 and 7 in Kramarz and Bond 2014) are related to the wear facets and orientation of lophids/lophs. We did not include them in our analysis because these characteristics are directly related to the degree of tooth wear, as newly available evidence demonstrates. The fully lophodont cheek teeth unquestionably characterize Pyrotheriidae and differentiate it not only from

other SANUs such as Xenungulata (e.g., *Carodnia*) and Notoungulata (*Notostylops*) but also from *Colombitherium* and *Proticia*. Indeed, no synapomorphy links *Colombitherium* and *Proticia*, which does not support a natural group Colombitheriidae as other authors proposed (Salas et al. 2006; Billet et al. 2010; Kramarz and Bond 2014).

Local geology and the geochronology of the Cañadón Pelado fossil-bearing level

In the study area, the antecedents of Cañadón Pelado did not account for the presence of sediments attributable to the Sarmiento Formation, much less the occurrence of mammal fossils (see Silva Nieto et al. 2005). Auspiciously, after several field trips to Cañadón Pelado since 2016, not only tuff sediments of the Sarmiento Formation were recognized there but also hundreds of mammalian fossil remains coming from two bearing-fossils levels (Fig. 1). According to a preliminary study, these mammal associations, given mainly by the presence of *Notopithecus* (in the lower level) and *Propyrotherium* (in the upper level), were correlated respectively with the Barrancan and Mustersan faunas, middle-late Eocene age (González Ruiz and Vera 2018; Vera et al. 2020a, b).

Given the geochronology data reported here, the sampled horizon 15 m below the *Propyrotherium* level bearing the dated zircons would have deposited at some time after 44.1 and before 37.5 Ma and more likely between 39.65 and 40.41 Ma (according to the weighted mean, 40.03 ± 0.38 Ma). Consequently, the age of the dated level falls within the range of 41.7–38.45 Ma reported for the Gran Barranca Member of the Sarmiento Formation at Gran Barranca, which contains the Barrancan fauna (Dunn et al. 2013). And it is older than the Mustersan fauna (included in both the Rosado and Lower Puesto Almendra members of the Sarmiento Formation at Gran Barranca; Ré et al. 2010), which may range from ca. 38.2 to 38 Ma (Dunn et al. 2013). The *Propyrotherium* level is surely somewhat younger than the estimated age of the dated level, but more sedimentological and stratigraphic evidence is needed to more precisely estimate the age of the *Propyrotherium* level.

Outside of Patagonia, the chronology of Cañadón Pelado can be correlated with the Eocene fossiliferous units of north-western Argentina (Salta Province), such as the upper levels of the Lumbrera Formation dated at 39.9 Ma (del Papa et al. 2010), and the base of the Quebrada Los Colorados Formation dated at 40.6 Ma (DeCelles et al. 2011), where a new pyrothere was recently reported (Fernández et al. 2021). *Propyrotherium* (a fragment of a tusk) was mentioned as well from the Antofagasta fauna of the Geste Formation (Catamarca Province, Argentina; López 1997), a unit dated between 37 and 35 Ma (DeCelles et al. 2007). However, the fragmentary condition of this specimen does not permit a precise identification, leaving it a highly doubtfully report (Reguero et al. 2008; García-López and Babot 2015). More recently, Kramarz et al. (2022) reported an isolated tusk and two isolated lower molars attributed to *Propyrotherium saxeum* from the Las Chacras Formation (Río Negro Province, north Patagonia) dated in 39.2 ± 2 Ma.

In summary, although *Propyrotherium* was previously considered to be restricted to the Mustersan age exclusively based on biochronological association, the available geochronological data documents that *Propyrotherium* is recorded from the Bartonian levels of the Sarmiento Formation, Chubut Province (40.03 ± 0.38 Ma at Cañadón Pelado, this paper) and Las Chacras Formation, Río Negro Province (39.2 ± 2 Ma, Kramarz et al. 2022). That is, it has a biochron much longer than previously thought, spanning with certainty from the Barrancan age and, tentatively, to the Tiguirirican age (see Kramarz and Bond 2014).

Conclusions

In this contribution, several aspects are worth highlighting. In one regard, we formally describe a new paleontological locality, Cañadón Pelado, from western Patagonia (Chubut Province, Argentina), where tuffaceous sediments of the Sarmiento Formation are recognized for the first time. An absolute age utilizing U–Pb zircon dating establishes an age of 40.03 ± 0.38 Ma (Bartonian) for a tuff level 15 m above the bed bearing the *Pyrotherium* specimens. This information is crucial because it not only provides a chronological framework for the fauna of Cañadón Pelado (where more than one hundred unpublished specimens of SANU, xenartrans, and metatherians were recovered) but also allows for establishing correlations with other calibrated middle-late Eocene faunas and units from Patagonia and other areas of Argentina and South America.

On the other hand, we describe the most complete mandible ever known and other isolated lower and upper teeth, of *Propyrotherium saxeum*, a scarcely known Eocene member of the highly peculiar SANU Pyrotheria. These specimens allow us to greatly improve the diagnosis of *P. saxeum*, describe its dental formula and new characteristics, and re-examine the specimens previously referred to this taxon by other authors. Based on that, we establish comparisons with other SANUs (e.g., pyrotheres and xenungulates) to evaluate the phylogenetic relationships of *Propyrotherium* with other pyrotheres.

Finally, this work adds a new report with chronological data for *Propyrotherium saxeum*, expanding its biochron from the Bartonian and its geographic distribution to the most western outcrops of the Sarmiento Formation in Chubut Province (Argentina).

Supplementary Information The online version contains supplementary material available at https://doi.org/10.1007/s00114-022-01810-z.

Acknowledgements We thank A. Taboada (CIEMEP) for providing important literature and unpublished data on the Cañadón Pelado locality; Puesto Blanco's owners for allowing us to work on their territory; M. Cárdenas (MACN) for preparing the specimen LIEB-PV 3200, and W. Dromaz, L. González Ruiz, G. Martin (CIEMEP), and E. Vasquetto (UNPSJB) for technical assistance and help in the field.

Author contribution B.V., conceptualization, formal analysis, funding acquisition, investigation, methodology, project administration, supervision, writing—original draft, writing—review and editing. M.F., formal analysis, investigation, writing—review. W.S. and N.B., formal analysis, methodology, visualization, writing—review and editing.

Funding This work was supported by Consejo Nacional de Investigaciones Científicas y Técnicas (CONICET PIP 2017–0767 to BV) and a CONICET-LA.TE ANDES Laboratory agreement.

References

Ameghino F (1888) Rápidas diagnosis de algunos mamíferos fósiles nuevos de la República Argentina. In: Torcelli AJ (ed) Obras Completas y Correspondencia Científica de Florentino Ameghino. 5. Taller de Impresiones Oficiales, Buenos Aires, pp 471–480

Ameghino F (1894) Première contribution à la connaissance de la faune mammalogique des couches à *Pyrotherium*. Bol Inst Geog Arg 15:603–622

Ameghino F (1901) Notices préliminaires sur des ongulés nouveaux des terrains Crétacés de Patagonie. Bol Acad Nac Cienc Córdoba 16:386–390

Ameghino F (1902) Línea filogenética de los proboscídeos. Anales Del Museo Nacional De Buenos Aires 3(1):9–43

Ameghino F (1904) Recherches de morphologie phylogénétique sur les molaires supérieures des ongulés. An Mus Nac Buenos Aires 3(3):1–541

Ameghino F (1906) Les formations sédimentaires du Crétacé supérieur et du Teriaire de Patagonie. An Mus Nac Buenos Aires 3(8):1–568

Ameghino F (1897) Mammifères crétacés de l'Argentine. Deuxième contribution à la conaissance de la faune mammalogique des couches à Pyrotherium. Bol Inst Geog Arg 18(4–6):406–429; (7–9):431–521

Anthony HE (1924) A new fossil perissodactyl from Peru. Am Mus Novit 111:1–4

Antoine PO, Billet G, Salas-Gismondi R, Tejada Lara J, Baby P, Brusset S, Espurt N (2015) A New *Carodnia* Simpson, 1935 (Mammalia, Xenungulata) from the early Eocene of northwestern Peru and a phylogeny of xenungulates at species level. J Mamm Evol 22(2):129–140

Billet G (2010) New observations on the skull of pyrotherium (Pyrotheria, Mammalia) and new phylogenetic hypotheses on south American ungulates. J Mamm Evol 17:21–59

Billet G (2011) Phylogeny of the Notoungulata (Mammalia) based on cranial and dental characters. J Syst Palaeontol 9:481–497

Billet G, Orliac M, Antoine P-O, Jaramillo C (2010) New observations and reinterpretation on the enigmatic taxon *Colombitherium* (?Pyrotheria, Mammalia) from Colombia. Palaeontol 53:319–325

Brocklehurst RJ, Crumpton N, Button E, Asher RJ (2016) Jaw anatomy of *Potamogale velox* (Tenrecidae, Afrotheria) with a focus on cranial arteries and the coronoid canal in mammals. PeerJ 4:e1906

Cerdeño E, Vera B (2017) New anatomical data on *Pyrotherium* (Pyrotheriidae) from the late Oligocene of Mendoza, Argentina. Ameghiniana 54:290–306

Chebli GC, Nakayama C, Sciutto JC, Serraiotto A (1976) Estratigrafía del Grupo Chubut en la región central de la provincia homónima. VI Cong Geol Arg, Actas 1:375–392

Cifelli RL (1993) The phylogeny of the native South American ungulates. In: Szalay FS, Novacek MJ, McKenna MC (eds) Mammal Phylogeny, vol 2. Placentals. Springer Verlag, New York, pp 195–216

Cohen KM, Finney SC, Gibbard PL, Fan J-X (2022) The ICS International Chronostratigraphic Chart Epis 36:199–204

Couto-Ribeiro G, Alvarenga H (2009) Primeiro registro de dentes de *Pyrotherium* para a Formação Tremembé, Bacia de Taubaté, SP. Reun An Soc Bras Paleontol, São Paulo, Abstr:21

Couto-Ribeiro G (2010) Avaliação morfológica, taxonômica e cronológica dos mamíferos fósseis da Formação Tremembé (Bacia de Taubaté), Estado de São Paulo, Brasil. Unpublished Ms thesis, Instituto de Biociências da Universidade de São Paulo, Brazil, pp 1–99

Coutode C P (1952) Fossil mammals from the beginning of the Cenozoic in Brazil. Condylarthra, Litopterna, Xenungulata, and Astrapotheria. Bul Am Mus Nat Hist 99:355–394

Croft DA, Gelfo JN, López GM (2020) Splendid innovation: the extinct South American native ungulates. Annu Rev Earth Planet Sci 48:259–290

de Muizon C, Billet G, Argot C, Ladevèze S, Goussard F (2015) *Alcidedorbignya inopinata*, a basal pantodont (Placentalia, Mammalia) from the early Palaeocene of Bolivia: anatomy, phylogeny and palaeobiology. Geodiversitas 37:397–634

DeCelles PG, Carrapa B, Gehrels GE (2007) Detrital zircon U-Pb ages provide provenance and chronostratigraphic information from Eocene synorogenic deposits in northwestern Argentina. Geol 35:323–326

DeCelles PG, Carrapa B, Horton BK, Gehrels GE (2011) Cenozoic foreland basin system in the central Andes of northwestern Argentina: implications for Andean geodynamics and modes of deformation. Tecton 30:TC6013. https://doi.org/10.1029/2011TC002948

del Papa C, Kirschbaum A, Powell J, Brod A, Hongn F, Pimentel M (2010) Sedimentological, geochemical and paleontological insights applied to continental omission surfaces: a new approach for reconstructing Eocene foreland basin in NW Argentina. J South Am Earth Sci 29:327–345

Dunn R, Madden R, Kohn M, Schmitz M, Strömberg C, Carlini A, Ré G, Crowley J (2013) A new high precision U-Pb chronology for middle Eocene-early Miocene South American Land Mammal Ages of the Sarmiento Formation, Gran Barranca, Chubut Province, Argentina. Geol Soc Am Bul 125:539–555

Fernández M, Fernicola J C, Bond M, Chornogubsky L, Zimicz N, Muñoz N A (2021) Primer Pyrotheria (Mammalia, Meridiungulata) de la Formación Quebrada de Los Colorados (Eoceno mediotardío), provincia de Salta, Noroeste Argentino. Congr Asoc Paleo Arg. Resum:116–117

Ferretti MP, Debruyne R (2011) Anatomy and phylogenetic value of the mandibular and coronoid canals and their associated foramina in proboscideans (Mammalia). Zool J Linn Soc 161:391–413

Feruglio E (1949) Descripción geológica de la Patagonia. I-III. Dirección General Yacimientos Petrolíferos Fiscales, Buenos Aires

Franchi MR, Page RFN (1980) Los basaltos cretácicos y la evolución magmática del Chubut occidental. Rev Asoc Geol Arg 35(2):208–229

García-López DA, Babot MJ (2015) Notoungulate faunas of northwestern Argentina: new findings of early-diverging forms from the Eocene Geste Formation. J Syst Paleontol 13:557–579

Gaudry A (1909) Fossiles de Patagonie: le *Pyrotherium*. Ann Paléont 4:1–28

Gehrels GE, Valencia VA, Ruiz J (2008) Enhanced precision, accuracy, efficiency, and spatial resolution of U-Pb ages by laser ablation–multicollector– inductively coupled plasma–mass spectrometry. Geochem Geophys Geosyst 9(3):Q03017. https://doi.org/10.1029/2007GC001805

Gelfo JN, López GM, Bond M (2008) A new Xenungulata (Mammalia) from the Paleocene of Patagonia, Argentina. J Paleontol 82:329–335
Goloboff PA, Farris JS, Källersjö M, Oxelman B, Ramírez MJ, Szumik CA (2003) Improvements to resampling measures of group support. Cladistics 19:324–332
Goloboff P, Farris J, Nixon K (2008) TNT, a free program for phylogenetic analysis. Cladistics 24:774–786
GonzálezRuiz LR, Vera B (2018) Mamíferos fósiles de la Formación Cañadón Pelado (Eoceno medio), Provincia del Chubut, Argentina. 31º Jor Arg Paleont Vert, Santa Clara del Mar, Buenos Aires. PE-APA 18(2):R76
Hoffstetter R (1970) *Colombitherium tolimense*, pyrothérien nouveau de la Formation Gualanday (Colombie). Ann Paléont 56:147–170
Kramarz A, Bond M (2014) Reconstruction of the dentition of *Propyrotherium saxeum* Ameghino, 1901 (Mammalia, Pyrotheria): taxonomic and phylogenetic implications. J Vert Paleont 34:434–443
Kramarz A, Bellosi E, Bond M, Forasiepi AM, Fernicola JC, Aguirrezabala G, Teixera de Rezende D (2022) Eocene mammals from volcaniclastic deposits of the Somun Cura Plateau: biostratigraphic implications for north Patagonia Paleogene. And Geo 49(2):238–272
Lesta PJ, Ferello R (1972) Región Extraandina de Chubut y Norte de Santa Cruz. In: Leanza AF (ed) Geología Regional Argentina. Academia Nacional de Ciencias Córdoba, pp 601–653
Loomis FB (1914) The Deseado Formation of Patagonia. Amherst College, Amherst, pp 1–232
López GM (1997) Paleogene faunal assemblage from Antofagasta de la Sierra (Catamarca Province, Argentina). Paleovert 26:61–81
Lucas SG (1986) Pyrothere systematics and a Caribbean route for land-mammal dispersal during the Paleocene. Rev Geol Am Cent, San José, Costa Rica 5:1–35
Maddison WP, Maddison DR (2018) Mesquite: a modular system for evolutionary analysis. Version 3.61. http://mesquiteproject.org
Nullo F (1983) Descripción Geológica de la Hoja 45c, Pampa de Agnia. Provincia de Chubut. Serv Geol Nac, Buenos Aires, Boletín 199:1–194
Nullo, Rivas OO (1971) Evolución de las comunidades de los vertebrados del Terciario Argentino. Los aspectos paleozoogeográficos y paleoclimáticos relacionados Ameghiniana. 7(3–4):372–412
Pascual R, Odreman Rivas O (1973) Las unidades estratigráficas del Terciario portadoras de mamíferos. Su distribución y sus relaciones con los acontecimientos diastróficos. V Cong Geol Arg, Actas 3:293–338
Patterson B (1942) Two Tertiary mammals from Northern South America. Am Mus Novit 1173:1–7
Patterson B (1977) A primitive pyrothere (Mammalia, Notoungulata) from the Early Tertiary of Northwestern Venezuela. Fieldiana, Geol 33:397–422
Ré GH, Bellosi ES, Heizler M, Vilas JF, Madden RH, Carlini AA, Kay RF, Vucetich MG (2010) A geochronology for the Sarmiento Formation at Gran Barranca. In: Madden RH, Carlini AA, Vucetich MG, Kay RF (eds) The paleontology of Gran Barranca: evolution and environmental change through the middle Cenozoic of Patagonia. Cambridge University Press, Cambridge, pp 46–58
Reguero MA, Croft DC, López G, Alonso RN (2008) Eocene archaeohyracids (Mammalia: Notoungulata: Hegetotheria) from the Puna, northwest Argentina. J South Am Earth Sci 26:225–233
Salas R, Sánchez J, Chacaltana C (2006) A new pre-Deseadan pyrothere (Mammalia) from Northern Peru and the wear facets of molariform teeth of Pyrotheria. J Vert Paleont 26:760–769
Sánchez-Villagra MR, Burnham RJ, Campbell DC, Feldmann RM, Gaffney ES, Kay RF, Lozsán R, Purdy R, Thewissen JGM (2000) A new nearshore marine fauna and flora from the early Neogene of northwestern Venezuela. J Palaeont 74:957–968
Scott WB (1913) A history of land mammals in the Western Hemisphere. Macmillan, New York, pp 1–693
Shockey BJ, Anaya F (2004) *Pyrotherium macfaddeni* sp. nov. (Late Oligocene, Bolivia) and the pedal morphology of the pyrotheres. J Vert Paleont 24:481–488
Silva Nieto DG, Márquez M, Ardolino A, Franchi M (2005) Hoja Geológica 4369-III. Paso de Indios. Provincia Del Chubut Boletín 267:1–164
Simpson GG (1935) Descriptions of the oldest known South American mammals, from the Río Chico Formation. Am Mus. 793:1–26
Simpson GG (1945) The principles of classification and a classification of mammals. Bul Am Mus Nat Hist 85:1–350
Simpson GG (1948) The beginning of the age of mammals in South America. Part 1. Bul Am Mus Nat Hist 91:1–232
Simpson GG (1967) The beginning of the age of mammals in South America. Part 2. Bul Am Mus Nat Hist 137:1–260
Simpson GG (1980) Splendid isolation: the curious history of South American mammals. Yale Univ. Press, New Haven, CT
Sláma J, Košler J, Condon DJ, Crowley JL, Gerdes A, Hanchar JMM, Horstwood SA, Morris JA, Nasdala L, Norberg N, Schaltegger U, Schoene B, Tubrett MN, Whitehouse MJ (2008) Plešovice zircon: a new natural reference material for U-Pb and Hf isotopic microanalysis. Chem Geol 249:1–35
Suero T (1948) Descubrimiento de Paleozoico superior en la zona extraandina de Chubut. Bol Inf Petr 25(287):31–48
Suero T (1953) Las sucesiones sedimentarias suprapaleozoicas de la zona extraandina del Chubut (Patagonia Austral, República Argentina). XIX Cong Geol Int 20:37–53
Suero T (1958) Datos geológicos sobre el Paleozoico superior en la zona de Nueva Lubecka y alrededores. Rev Mus De La Plata 5(30):1–28
Tabuce R, Jaeger JJ, Marivaux L, Salem M, Bilal AA, Benammi M, Chaimanee Y, Coster P, Marandat B, Valentin X, Brunet M (2012) New stem elephant-shrews (Mammalia, Macroscelidea) from the Eocene of Dur At-Talah, Libya. Palaeontology 55:945–955
Turner JC (1983) Descripción geológica de la Hoja 44d, Colan Conhué. Serv Geol Nac, Boletín 197:1–178
Vera B (2016) Phylogenetic revision of the South American notopithecines (Mammalia, Notoungulata). J Syst Palaeont 14:461–480
Vera B, Cerdeño E (2014) New insights on *Antepithecus brachystephanus* Ameghino, 1901 and dental eruption sequence in 'notopithecines' (Mammalia, Notoungulata) from the Eocene of Patagonia, Argentina. Geobios 47:165–181
Vera B, Fornasiero M, Del Favero L (2020a) New data on *Carodnia feruglioi* (Carodniidae, Xenungulata) from the early Eocene of Patagonia (Argentina). Ameghiniana 57(6):566–581
Vera B, Ciancio M, Vasquetto E, Martin G, González Ruiz L (2020b) Nueva asociación de mamíferos eocenos en el oeste del Chubut: avances y resultados preliminares. Reunión de Comunicaciones de la Asociación Paleontológica Argentina. PE-APA 20(1):29
Wiedenbeck M, Hanchar J, Peck W, Sylvester P, Valley J, Whitehouse M, Kronz A, Morishita Y, Nasdala L, Fiebig J, Franchi I, Girard J-P, Greenwood R, Hinton R, Kita N, Mason PRD, Norman M, Ogasawara M, Piccoli R, Zheng Y-F (2004) Further characterization of the 91500 Zircon Crystal. Geostand Geoanal Res 28:9–39